



# Advances in nanomaterials for phosphates removal from water and wastewater: a review

Assaad Hassan Kassem<sup>1</sup> · George M. Ayoub<sup>1</sup> · Ramez Zayyat<sup>1</sup>

Received: 24 August 2021 / Accepted: 9 April 2022 / Published online: 11 May 2022  
© The Author(s), under exclusive licence to Springer Nature Switzerland AG 2022

## Abstract

Phosphate is considered one of the major natural nutrients associated with the sustainment of life on earth. However, its presence in excessive amounts in water bodies may induce adverse environmental impacts. Among the various treatment techniques practiced for the removal of phosphate from aqueous solutions, adsorption is considered the most effective. Compared to other phosphate treatment methodologies, adsorption is characterized by its high removal efficiency and economic feasibility. Accordingly, many sorbents, specifically nano-sorbents, have been synthesized and modified for application in the removal of phosphate from water. Out of the numerous utilized nano-sorbents, metal oxides and chitosan have shown to be very effective sorbents when applied for the removal of phosphates from aqueous solutions. The present study covers a review of recent developments and applications of nano-sorbents, in particular the fore-mentioned nano-sorbents, for the removal of phosphates while discussing the removal mechanisms associated with their application. A critical assessment related to the recent studies and their shortfalls is also explored.

**Keywords** Phosphate · Adsorption · Nano-Sorbents · Chitosan · Metal Oxides

## Introduction

Urbanization and industrialization lead to water quality deterioration [1], wastewater resulting from agricultural, industrial, and domestic water usages are discharged into water bodies thus conveying hosted contaminants and polluting the environment and the limited water resources [2]. Phosphate is considered one of those contaminants, where despite its vitality for living species as a nutrient [3], excessive amounts discharged into streams and rivers would lead to the deterioration of water quality [4–7].

The presence of phosphorous can be of tremendous use to industries, agriculture, etc.; however, the presence of such a compound in water bodies and wastewater effluents pose a threat to human health and the entire environment [8]. High concentrations of phosphorous in water bodies are mainly present in the form of phosphate, which consequently affect human and environmental health [9–11]. The increased use of phosphate-based fertilizers is a direct effect of high-input

of modern agricultural performs. In the USA, numerous water bodies (42 percent of lakes and 66 percent of rivers) are adversely impacted by the excess of phosphorus concentration (with  $> 30 \mu\text{g PO}_4^{-3}$ ) [8]. At concentrations exceeding 0.02 mg/l, phosphates can cause eutrophication marked by massive algal growth which in turn leads to higher water turbidity [12], decrease in oxygen levels [13], production of bad odors, and harming aquatic life [14]. Due to these deleterious impacts, interest in devising methods for phosphate removal from aqueous solutions has been growing and as a result many methods have been developed including biological treatment [15], chemical precipitation [16, 17], and adsorption [18–22]. Even though biological treatment with activated sludge removes most phosphates present in water, it is not effective in removing trace level phosphates due to the reduction of microbial metabolism. In addition, the sludge generated due to chemical and biological treatments is considered as a major nuisance. Physical methods, such as reverse osmosis and electrodialysis, have been identified as too inefficient or costly [23]. Compared to other treatment techniques, adsorption is the most convenient method due to its economic feasibility and high phosphate removal efficiency even at the nanoscale [24–26].

✉ George M. Ayoub  
gayoub@aub.edu.lb

<sup>1</sup> Departmentt of Civil and Environmental Engineering,  
American University of Beirut, Beirut, Lebanon

The use of nanomaterials in engineering applications is gaining huge popularity [27], both natural and synthetic nano-based polymers are employed in the synthesis of neuron-inspired network materials, tunable sensing materials [28], healing products, and energy storage materials [29]. The use of nanomaterials that are low-cost, facile to manufacture, highly abundant in nature, and easy to scale-up paves the way to reach green electrocatalysts and, in turn, opening horizons for the development of innovative clean energy technologies [30, 31]. With the increased risk of water contamination, the development of cleaner energy technologies becomes imperative. To that end, multiple carbon core–shell-based nanocatalysts made from readily available materials were developed for the treatment of organic matter present in water [32]. According to Ahsan et al. [33], the eco-friendly catalytic nano-systems are advantageous due to its possibility of control over the electron transfer processes at the metal/carbon interfaces under various experimental conditions, ultimately controlling their trifunctional catalytic performances.

Many sorbents have been developed for phosphate removal from water and wastewater [34]. The most widely and traditionally used sorbent is activated carbon. The use of cheaper and more readily available materials for absorption has been excessively studied in the literature. Clays have been used for thousands of years and continue to be among the leading industrial material that are naturally available, earthy and fine-grained [35]. Another alternative is the use of surface-modified biochar which is classified as cheap, non-toxic and easy to obtain, with high specific surface areas, and large pore volumes, allowing the chance of physio-sorption and hydrophobic interaction and electrostatic adsorption with contaminants proficiently [36]. Materials such as chitosan have been modified structurally or chemically with metal, metal oxides, and other functional groups to assist it in phosphates removal from water where removal capacity exceeded 300 mg of phosphates per gram of chitosan [37–41]. Semi-metal and metal oxides, solely or in mixture, have also aided in the removal of phosphate from water reaching high removal efficiency of 100% and more than 900 mg/g as an adsorption capacity according to some studies [18, 42, 43]. Additionally, nanoscale zero-valent iron was found to be an effective adsorbent of phosphates in water [44, 45].

The aim of this manuscript is to conduct a review of recent advances in the use of nano-sorbents for phosphate removal. In this context, chitosan, metal oxides, combinations of metal oxides and zero-valent iron are reviewed in this paper. Besides, this review paper explores the mechanisms of removal of phosphate using the nanomaterials under study. The importance of phosphate removal and the surge in nanotechnology applications in water treatment calls for perpetual literature reviews that can help

in assessing recent advances and identifying gaps in this field.

The significance of such work is to revisit previously reported modification on metal oxides and chitosan-based nanomaterials to point out conditions that impact successful phosphate removal from water matrices. Furthermore, this review classifies the reported materials by type, thus showing a wide overview of the diversity of adsorbents and their levels performance that have been prepared so far.

## Metals, semi-metals, and metal oxides removal: experimental findings and main removal mechanism

Generally, metals like iron, semi-metals like graphene and metal oxides similar to iron oxides, magnesium oxides, aluminum oxides, zinc oxides and titanium oxides and combinations thereof are used as adsorbents that aid in the removal and recovery of various materials and their compounds with phosphates being precisely discussed in this paper [46, 47]. The advantages offered by these sorbents include their highly porous nature, high stability across wide ranges of pH, temperature, and their economic feasibility [48]. Their performance differs greatly depending on adsorbent dosage, ionic interaction, surface area, contact time, temperature and pH; however, mainly all have achieved high removal efficiencies [49].

### Aluminum oxide

Several attempts at using nanomaterials in the removal of phosphates from water and wastewater have been reported. One example is related to the utilization of nano-alumina as an adsorbent in a batch experiment setup. Parameters including contact time, pH, adsorbent dosage, temperature, agitation rate and initial phosphate concentration played an important role in determining the adsorption rate, with pH being the most important due to the fact that the adsorption mechanism relies on the amount of -OH groups that will be attracted to the protons and are thus adsorbed [50, 51]. Results indicated that the pH level at which nano-alumina showed the highest adsorption (98%) was 8.1 with a contact time of 90 min [52].

Kumar et al. [53] also proved that phosphates are considered competing species in the presence of nanomaterial, a study conducted by Mor et al. [54] in order to compare between the efficiency of two nanomaterials of different natures, one possessing an amorphous nature (activated carbon) and the other possessing a crystalline nature (nano-alumina) but both share a porous nature and are thus classified as good adsorbents. Time, pH, adsorbent dosage are major

factors that influence the removal efficiency in this batch-mode experiment, where experimental results exhibited a higher removal efficiency of nano-alumina (up to 100% in 90 min and pH 6) in comparison to activated charcoal (90.2% in 120 min and pH 6).

This compares with the study that was presented by Yadav et al. [52], which has shown that adsorbents favored lower pH levels and achieved optimal removal rates when phosphate is used as an adsorbate. Kinetics of the reaction were explored to show that phosphate adsorption follows a monolayer adsorption process for both nanomaterials [55].

## Zinc oxide

Zinc oxide is also a notable candidate that has proven its ability to remove various nutrients like phosphates and nitrates from water and wastewater [56]. An attempt was made by Cervantes-Avilés, Cuevas-Rodríguez [57] to assess the removal of orthophosphates using zinc oxide nanoparticles on activated sludge and filtered wastewater, whereby in both control groups of water the removal was 78 and 82%, respectively. These results were consistent with other long-term adsorption studies [58]. Though the removal mechanisms remain uncertain, however they could be due to crystallization and precipitation processes that befall phosphate compounds in the presence of zinc oxide nanomaterial upon forming  $Zn_3(PO_4)_2$ , which is a stable product [59]. Another study that explored the applicability of layered zinc hydroxide in the removal of phosphorus materials resulted in 95% removal which is attributed to the exchangeable anionic behavior within the layered structure [60].

It is still unclear how zinc oxides may assist in the removal of phosphates ( $PO_4^{3-}$ ) in the presence of living organisms, like green algae, knowing that these oxides might induce toxic effect onto living organisms, as most studies have been conducted to test the zinc oxides unaccompanied, or in combination with other nanomaterials [61–64]. The impact of zinc oxide nanoparticles on the removal of phosphate in the presence of green algae (*Chlorella vulgaris*) was examined, where  $PO_4^{3-}$  removal got accelerated with the presence of high zinc oxide nanoparticles due to the interaction between  $PO_4^{3-}$  and  $Zn^{2+}$  that were dissolved from zinc oxide nanoparticles forming crystallites and eventually leading to sedimentation [65, 66].

## Titanium oxide

Titanium oxides have shown their capability to remove various nutrients, metals and replace other nanomaterials like zirconium oxide due to its higher efficiency when acting as an adsorbent [67–69]. A drawback of various studies is that

they missed out on determining the recovery capabilities of the process. It is crucial when studying the removal efficiency of a certain nanomaterial to also determine the ability of its recovery as well as its byproducts since it might result in the production of even more complex materials [70].

In a study reported by Lee et al. [48], the authors investigated the adsorptive capabilities of titanium oxide and their abilities in phosphorus recovery. As titanium oxide is a porous nanomaterial, it possesses good potential as an adsorbent since it concedes ion exchange on its surface [22]. pH and temperature have shown to affect the removal efficiency whereby the most suitable pH values for phosphate removal were observed to be between the range of 3–7. Higher values tend to disturb the exothermic process of adsorption.

In a study conducted by Rad et al. [71], nano-titanium oxide, being an oxidizer, was applied as a thin cover over a pond body that contained tropical storm water exposed to natural ultraviolet rays (UV). The use of nano-titanium resulted in improving the storm water outflow quality by 57% in a time laps of 3 weeks, while the orthophosphate group was reduced by 83%. With the aid of ultraviolet rays, the pond was converted into a photocatalytic reactor where the reactions resulted in the formation of positive holes in the nanocomposite which could react and adsorb the pollutant.

This removal efficiency can be optimized by experimenting with various adsorbent dosages. An attempt at utilizing titanium oxide composite in combination with polyaniline in order to adsorb phosphates from wastewater was performed by Wang et al. [72]. The study revealed that this composite possesses high stability and an adsorption efficiency reaching 98% in 60 min within a wide pH spectrum (1–6). This manifestation was attributed to the presence of protonated amino groups in the composite whereby titanium oxide acted as a binding force via electrostatic interaction with phosphates. This procedure has the advantage of being applied in larger scale treatment processes.

## Iron oxide

Iron-based nanoparticles have been used widely as an adsorbent to remove various nutrients and dyes from wastewater [73–75]. Table 1 presents the most recent published articles for phosphate removal using iron oxides. In a study performed by Cao et al. [76], iron oxide nanoparticles reactivity was improved by incorporating a stabilizer (cetyltrimethylammonium bromide, CTAB) which greatly improved the removal efficiency of phosphate. The reactions were dependent on pH, contact time, dosage of phosphate and the composite as the results demonstrate that equilibrium data fitted well the Langmuir isotherm model. The removal activity occurred at different stages, slow and rapid with

**Table 1** Research on phosphate removal using Iron oxides

Iron Oxide	Type of Water	pH	Temperature	Adsorbent Dose	Contact time	Equilibrium Isotherm	Adsorption Capacity	Treatment method	Removal Efficiency
Iron oxide nanoparticle + cetyltrimethylammonium bromide [76]	Stock Solution + Deionized water	1.6	308 K	1 mg/l	120 min	Langmuir	9 + 1 mg/g	Batch experiment	97.30%
Ferrate(VI) [77]	Stock solution & wastewater	7	Room temperature	Fe/P mass ratio to 5:1	30 min	–	143.4 mg/g	in-situ and ex-situ experiments	100%
lanthanum oxide-Fe <sub>3</sub> O <sub>4</sub> @SiO <sub>2</sub> core/shell magnetic nanoparticles [78]	Stock solution & wastewater	5–9	Room temperature	> 0.2 g/l	10 min	Langmuir	27.8 mg/g	Adsorption experiment	99%
Bay-oxide	Lake water	< 9.5	21 °C	5 g/l	0.75 h	Langmuir	37.74 mg/g	Batch,	–
Bay-oxide-Mn nanoparticles		< 10.4		(Batch experiment)	0.75 h		30.96 mg/g	equilibrium, and	
Bay-oxide-AgI nanoparticles		< 7.3			0.75 h		25.52 mg/g	column experi-	
Bay-oxide-AgII nanoparticles [79]		< 10.5			1 h		38.8 mg/g	ments	
fibrous ion exchanger impregnated with nanoparticles of hydrated ferric oxide [80]	Stock Solution + Milli-Q water	6–8.5	21.1 °C	0.05 g/25 ml	24 h	Langmuir	16,212 mg/g	Batch and column experiments	–
(granular and fibrous) impregnated with nanoparticles of hydrated ferric oxide [81]	synthetic phosphate aqueous solution and wastewater secondary treated effluent	13.2	–	Batch experiment 3.4–3.5 g/7 l Column experiment	2 min column experiment	Langmuir	163 mg/g	Column experiment	–
iron oxide nanoparticles -cetyltrimethylammonium bromide-Eucalyptus leaf extract [82]	Diluted stock solution	–	25 °C	3.5 g/l 2 g/l	2 ml/min 60 min	–	–	–	95%

dual reaction of inner sphere complexing and electrostatic attraction taking place. The modified composite possessed two active sites (hydroxyl group on iron oxide and positively charged CTAB) resulting in increased efficiency in the removal of phosphates onto the active sites of the iron oxide.

Iron in various forms can have high removal efficiencies of nutrients; this was investigated by Kralchevska et al. [77] where Ferrate (VI) was selected for use as an adsorbent due to it being a strong oxidizing agent, environmentally friendly, as well as its recovery potential after being used in wastewater treatment. Ferrate has the advantage of having highly accessible active sites where the removal mechanism occurs solely by surface sorption at near neutral pH; making Ferrate (VI) a promising composite to be well utilized in this domain [83, 84].

Lai et al. [78] reported on the adsorption of phosphate from water by easily separable Fe<sub>3</sub>O<sub>4</sub>; in this study, a 99% phosphate removal was reported to take place in under 10 min. The authors further suggested that complete removal can be achieved in the future with the help of a NaOH solution. The composite used in the experimental work was composed of hydrous lanthanum oxide functionalized on the surface of Fe<sub>3</sub>O<sub>4</sub>@SiO<sub>2</sub> core/shell magnetic nanoparticles (Fe–Si–La), where the best removal performance was observed at a pH range of 5–9. These results are attributed to the surface speciation of oxides that contributed to the removal of phosphates. In addition to that, Fe–Si–La has a great potential because of its high stability even in the presence of other anions like chloride and nitrate.

Iron oxide-based sorbents have shown great potential in the removal of various ions. The adsorptive behavior of several iron composites among which are Bay-oxide E33 (E33), E33 coated with manganese (E33/Mn) and silver coated E33 (E33/AgI and E33/AgII) were investigated [79, 85, 86]. Chemisorption was found to be the main adsorption mechanism, which was divided into two phases, the first occurred rapidly and was delineated by film diffusion and the second transpired slowly through intra-particle diffusion. It was observed that E33/AgII had a slightly higher adsorptive capacity when compared to unmodified E33 implying that E33 had a weaker surface which can be enhanced through the process of combining it with other nanoparticles [87].

You et al. [80] endeavored to expand the functions of iron oxide as a sorbent by generating a selective sorbent for phosphate species which was a hybrid fibrous exchanger having hydrated ferric oxide nanoparticles abbreviated as (HFO). HFO had assets over other iron oxides delineated by its substantial mechanical strength and durability. The removal of phosphate anions took place by interacting with the existing Fe–OH group through the replacement of the hydroxyl group. Iron oxide nanoparticles performance can be enhanced by incorporating other elements [45, 88]. In this context, Gan et al. [82] studied the effect

of cetyltrimethylammonium bromide (CTAB) on the morphology of iron oxide nanoparticles where results showed that CTAB improved the aggregation of iron oxide nanoparticles and their dispersion thus enhancing its reactivity. Where electrostatic interaction occurred between CTA<sup>+</sup> and phosphate anions, a complex was formed; suggesting that CTAB is a stabilizing agent and an enhancer for removal of phosphates when added to iron oxides.

In another study conducted by You et al. [81], hybrid anion exchangers, containing hydrated ferric oxide nanoparticles, were used due to their selectivity for phosphate species. The combination gave greater mechanical strength and durability while achieving 90% removal of phosphates from wastewater following an interaction between phosphate groups and  $\cong\text{Fe}(\text{OH})$  which existed on the surface. The hybrid anion exchanger showed higher selectivity toward phosphates while neglecting other ions like nitrate, sulfate and chloride; it also had an added advantage where its showed high reusability rates after five sorption cycles.

## Magnesium oxide

Table 2 summarizes all recent work conducted on phosphate removal from water and wastewater using magnesium oxides. While studies show that magnesium oxide (MgO) has high affinity for phosphate species, enhancing the potential of MgO is a promising step that will lead to more efficient phosphate abstraction [89]. This was investigated by Jung, Ahn [90] where MgO/biochar was electrochemically modified using an electrolyte (MgCl<sub>2</sub>) and graphite electrode-based electric field to enhance the porosity of the composite. Results and analyses showed that the composite exhibited a highly enriched crystalline structure with high adsorption properties; though the mechanism of action remains unknown authors suggested further investigations to determine the process of adsorption.

Ahmed et al. [43] replicated the electrochemical enhancement process using a hydrothermal procedure, whereby magnesium oxide pores were synthesized by hydrothermally adding hexamethylene tetramine (HMT) to MgO, resulting in superior adsorption results. The kinetic and isotherm analysis underscored that the process of adsorption occurred physically and chemically, where negatively charged phosphates were attached onto the MgO surface. The authors suggested that porosity of MgO can be modified and regulated by adjusting the feed ratio of both HMT and Mg<sup>2+</sup>. Ma et al. [95] also hydrothermally synthesized magnesium oxide nanoparticles in several shapes which showcased great performance in removing phosphate.

The physical structure of the nanocomposite used to remove nutrients plays an important role in removal efficiency, since it delineates the surface area available for

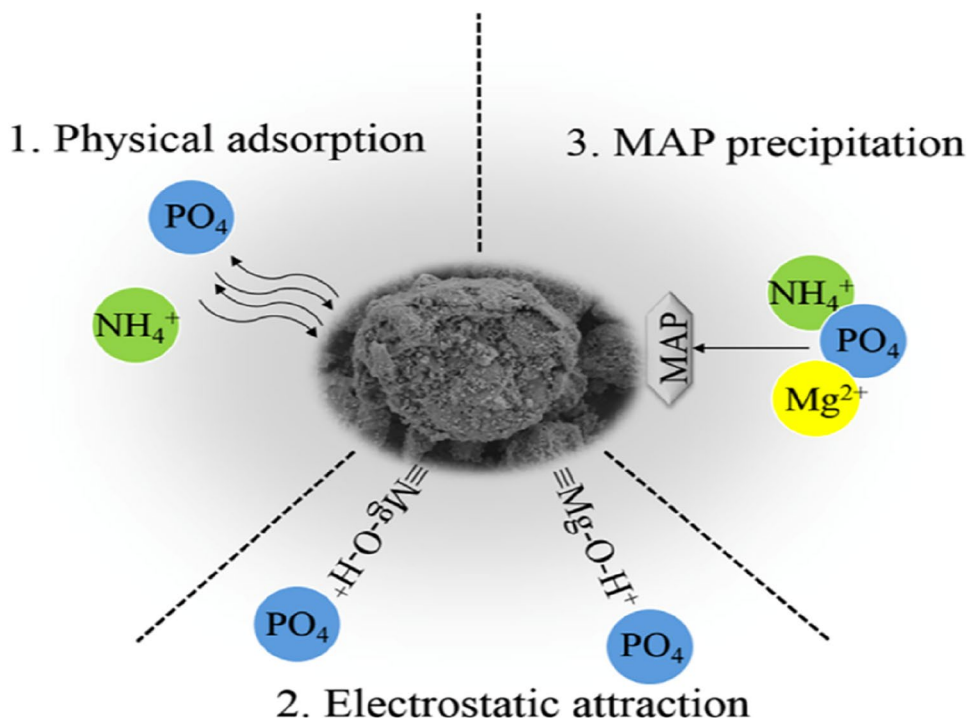
**Table 2** Research on Phosphate Removal Using Magnesium Oxides

Magnesium Oxide	Type of Water	pH	Temperature	Sorbent dose	Contact time	Equilibrium isotherm	Adsorption capacity	Treatment method	Removal efficiency
MgO nano-composites/biochar [90]	Phosphate solution		20 ± 2 °C	0.05 g/50 ml	48 h	Langmuir–Freundlich	620 mg/g	Batch experiment	
Mesoporous magnesium oxide modified diatomite [91]	Artificial stock solutions	7	25 °C	0.3 g/l	2 h		160.94 mg/g	Batch experiment	
Porous magnesium oxide prepared by hexamethylene tetramine [43]	Phosphate solution	5	30 °C	10 mg/100 ml		Freundlich	236 mg/g	Batch experiment	
MgO-impregnated porous biochar [92]	sodium phosphate monobasic monohydrate in DI water and swine wastewater	4	22.5 ± 0.2 °C	0.05 g/50 ml	1 h	Langmuir	398 mg/g	Batch experiment	> 99.1%
MgO supported palygorskite [72]	wastewater	9	–	0.6 g/l	3 h	–	69.8 mg/g	Batch experiment	
hierarchically porous magnesium oxide [93]	Phosphate solution	5	25 °C	0.01 g/0.1 l	5 h	Langmuir	478.5 mg/g	Batch experiment	
MgO-modified diatomite [92]	simulated nutrient wastewater	7	–	0.3 g/l	12 h	–	–	Batch experiment	–
Na and K zeolites and magnesium oxide [94]	anaerobic digestion side streams	9.5	–	MgO (Mg/P (3:1)) and using 20.7 g Na-zeolite/L in a single addition stage of both reactive sorbents	> 3 h	Nonlinear adsorption isotherm	–	Stirred reactor experiments	> 99%
Mgo nanowires [95]	Phosphate stock solution	11	–	10 mg/5 ml	–		962 ± 8.6 mg/g	Batch experiment	

contact with the pollutant. Xia et al. [91] manipulated the structure by creating a mesoporous magnesium oxide on diatomite, where diatomite is an abundant rock formed from microfossils of diatoms adding value to the composite due to its high porosity and thermal stability (Fig. 1). Experimental results demonstrate that the composite achieved high

removal rates at a wide range of pH (3–9), where pH had a major impact on the struvite crystallization, which is a product of phosphate adsorption [96]. The removal process is a result of physical adsorption where the shape of the composite was enhanced thus improving physical contact and electrostatic attraction, whereby MgO in solution becomes

**Fig. 1** Proposed mechanism of removal of phosphate using MgO-Diatomite [91]



protonated consequently attracting all negatively charged phosphate species [97, 98].

Magnesium oxide removal efficiency was enhanced by impregnating it in porous biochar [99]. Analysis of the results shows that the modified composite formed carbon nanotube-like structure and MgO flakes; the process of rapid adsorption occurred through struvite crystallization and electrostatic interactions between phosphate anions and the positively charged composite surface [100–102].

Further studies have been performed to exploit the properties of magnesium oxide where Wang et al. [103] synthesized an adsorbent of MgO supported by palygorskite (MgO-PAL). This composite was characterized by achieving high removal rates of phosphate resulting from the formation of several precipitates known as struvite,  $\text{Mg}(\text{OH})_2$  and  $\text{Mg}_3(\text{PO}_4)_2$ , through adsorption on the protonated surface of magnesium oxide palygorskite. Additionally, Ahmed et al. [93] successfully engineered a hierarchically porous magnesium oxide composite aimed at maximizing surface area to allow more pollutant adsorption. Adsorption occurred through physical contact and resulted in forming magnesium hydrogen phosphate and magnesium phosphate. This method depicts a procedure that can be adopted in industrial applications due to its economic feasibility (low-cost) [104].

To achieve complete stabilization of phosphates in a medium using magnesium oxide, system operation needs to be optimized in addition to forming a suitable MgO nanocomposite. Hermassi et al. [94] aimed to find the most suitable operative conditions while using a blend of reactive sorbents consisting of potassium zeolite, sodium zeolite and

magnesium oxide. Under alkaline conditions, phosphate ions precipitated with magnesium ions thus contributing to its stabilization in the form of bobierite. An additional advantage related to this experiment is that recovery procedures could generate various stable nutrients which can be used later in agricultural applications; a procedure that is environmentally sustainable [105].

## Graphene oxides

Graphene oxide is being and will be applied in several nanotechnological applications due to its unique physicochemical properties [106–108]. Graphene oxide is a two-dimensional carbon-based material with carboxyl, epoxy, and hydroxyl groups attached to its edges and surface [102]. Its functional groups and its hydrophilicity are the key factors for graphene oxide application in water sanitation [109–111]. Graphene oxide was also used for phosphate removal from water and wastewater but mostly in conjugation with other metal oxides which will be discussed in another section [99, 112, 113]. However, Xu et al. [42]. worked on graphene oxide as a sole sorbent for phosphate and europium removal from nuclear wastewater and studied the co-removal processes as a function of contact time, pH, and temperature. The sorption process fitted well the Langmuir sorption isotherm, while the presence of europium increased the electrostatic potential on graphene oxide aiding phosphate adsorption at an optimal pH 5.9–9, temperature 293 K, and contact time of 1 h.

## Zero-valent iron

Zero-valent iron has been widely used to remove heavy metals, organic and inorganic compounds because it exhibits large surface area making it apposite for adsorption [114, 115]. Table 3 presents recent studies reported on phosphate removal using zero-valent iron, and Fig. 2 demonstrates the main mechanism of removal and the effect of aging on adsorption capacity.

Chen et al. [112] utilized starch stabilized zero-valent iron nanoparticles to remove phosphate from a prepared solution using a batch experiment. Analysis showed that

starch assisted particles to aggregate leading to an increase in reactivity and surface area, where the presence of interfering ions had little to no effect on the adsorption but changes in temperature and pH had a significant impact. The main mechanism of action involved surface adsorption where OH groups present in starch stabilized the zero-valent iron. The phosphate species that had the highest affinity to the nanocomposite was  $\text{HPO}_4^{2-}$ .

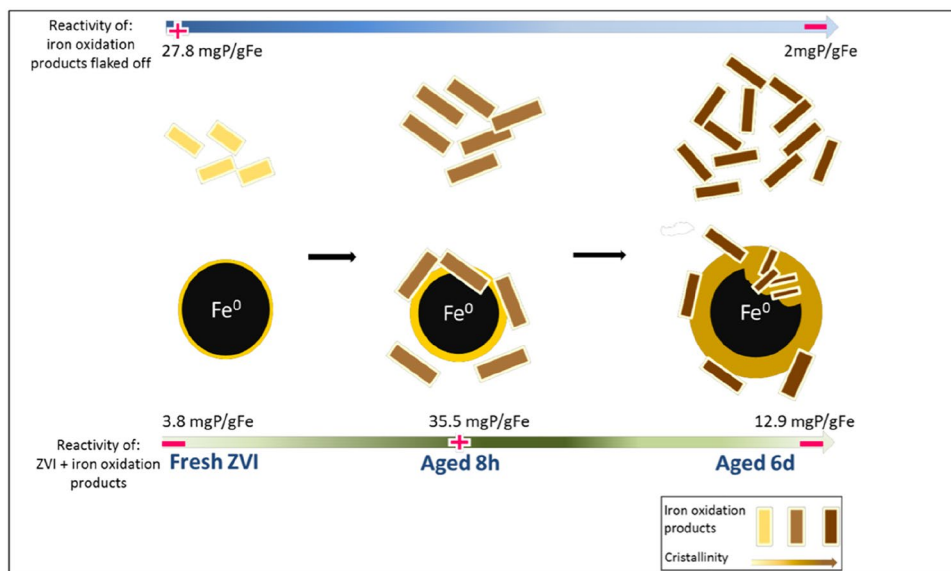
Another manipulation of zero-valent iron nanoparticles (ZVINPs) that resulted in key magnetic properties was performed by Singh, Singh [116] whereby magnetite ( $\text{Fe}_3\text{O}_4$ ) was used to stabilize zero-valent iron nanoparticles. In addition to magnetic properties, it supplied ZVINPs with

**Table 3** Research on phosphate removal by Zero-Valent Iron

Zero-Valent iron	Type of Water	PH	Temperature	Dose	Contact time	Equilibrium Isotherm	Adsorption capacity	Treatment method	Removal efficiency
Starch stabilized zero-valent iron [44, 116]	Phosphate solution	12	10 °C	1 g SNZVI per 100 g/L of phosphate	200 min	Langmuir	322.39 mg/g	Batch sorption	81.29%
$\text{Fe}_3\text{O}_4$ -Zero-Valent iron	Phosphate solution	3.5	49.2 °C	0.4 g L <sup>-1</sup>	2 h	–	164.92 mg/g	Batch sorption	99.2%
zero-valent iron supported on treated activated carbon [14]	phosphate solution	7	25 ± 2 °C	2:1 AC to nZVI	2 h	Langmuir	1.75 mg/g	Batch sorption	Batch II: > 60%
Zero-Valent iron/sand bed reactor	phosphate solution	7.0 ± 0.2	20 ± 3 °C	17 g/L	72 min	–	52 mg/g	Column adsorption	Batch III: > 90%
Zero-valent iron with copper chloride [117]	phosphate solution	12	25 ± 0.5 °C	250 mg/250 L	2 h	–	50 mg/g	Batch sorption	60%
Pectin-nanoscale zero-valent iron [118]	phosphate solution	5	25 °C	1 g/l	200 min	Langmuir	277.38 mg/g	Batch experiment	–
zero-valent iron activated persulfate [119]	Stock solutions and Wastewater	pH ≤ 6	25 °C	0.5 g/l	60 min	Freundlich	–	Batch experiment	91%
zero-valent iron [120]	Phosphate solution	7 ± 1	20 ± 3 °C	2.5 g/l	8 h	–	35 mg/g	Batch experiment	–
Nanoscale Zero-valent iron [45]	Phosphate solution	6.3	293 K	0.5 g/l	–	–	16 mg/g	Batch experiment	99.9%
								Column experiment	



**Fig. 2** Mechanism of removal of phosphate from aqueous solution and aging factor effects [120]



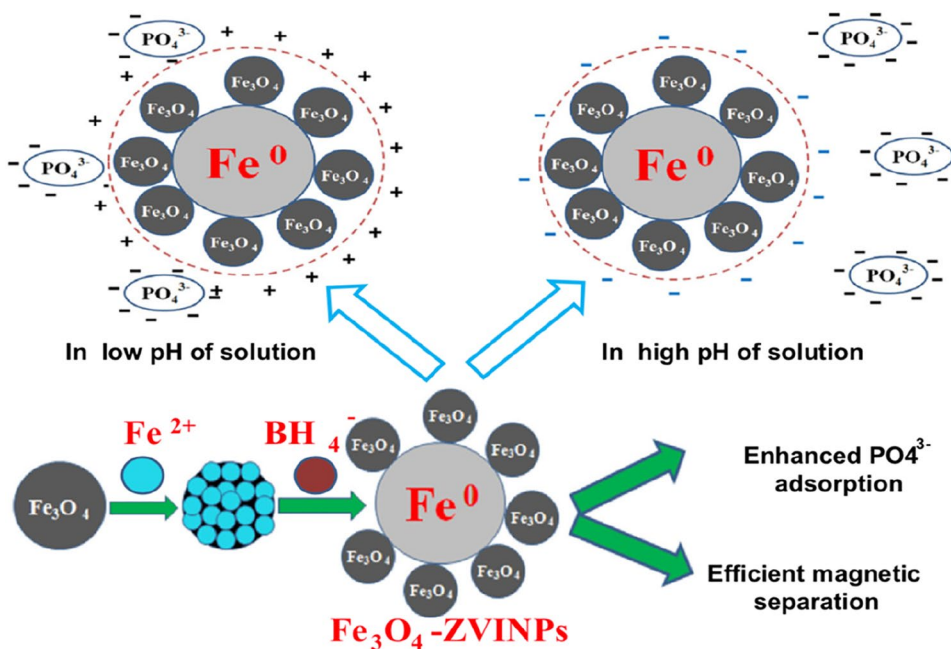
a larger surface area, reduced agglomeration of particles and enhanced removal efficiency [121–123]. Adsorption occurred through physical contact and chemical precipitation. Analysis showed that the presence of ions did not interfere with the process while pH had the highest impact on removal because it sets the surface charge of the adsorbent. At optimal pH,  $\text{Fe}_3\text{O}_4$ -ZVINPs acquires a positively charged surface thus attracting negatively charged phosphates via electrostatic attraction rendering magnetite ( $\text{Fe}_3\text{O}_4$ ) an effective removal method (Fig. 3) [124].

Activated carbon is another adsorbent of added value due to its sorption capabilities, especially when utilized in combination with ZVINPs [14, 125]. When zero-valent iron is

utilized solely, it faces oxidative issues, and activated carbon used alone is subject to poor diffusion. Studies have shown that when these two composites are integrated, they prevent agglomeration and enhance their hydraulic conductivity by attracting more anions [126, 127].

Activated carbon represents a support system to zero-valent iron nanoparticles at which they are immobilized and trapped on the surface of AC in addition to acting as an electron accepting composite, where physical adsorption is the main sorption mechanism [72, 128]. This must be conducted with a suitable concentration of AC, because under increased AC concentration the process of adsorption is hindered due to the reduced contact to nano-zero-valent

**Fig. 3** pH Effect on removal of phosphate anions from aqueous solution using iron oxide-zero-valent iron nanoparticles [116]



iron (nZVI). The presence of nitrates in solution aid in the adsorption of phosphate as they reduce nZVI to form Iron(I) hydroxide and Iron (II) hydroxide, thus enhancing adsorption kinetics [14, 117].

Column adsorption is one method that maximizes the chances for the pollutant to encounter the adsorbing medium [129, 130]. Sleiman et al. [131] designed a zero-valent iron (ZVI)/sand packed column to test its efficiency in removing phosphate, where the sand represented a support material for ZVI [132]. The effect of column conditioning and aging on the adsorption process was tested. The results showed that a column that has aged for 1 day displayed the maximum removal efficiency when compared to 5 and 10 days of aging. This was attributed to the fact that increased conditioning and aging leads to saturating the composites in advance of the experiment and consequently minimizing the adsorbent surface area. The process of adsorption occurred through phosphorus trapping and was measured as a function of oxygen and oxidized outlet which in turn was measured as a function of pH [131]. Surface adsorption occurred after oxygen and water within the solution has formed compounds (Fe–O & Fe–OH) which induced phosphates forming P-OH and O-P [133, 134].

It is not necessarily the ZVI, or the element added to it that will function as an adsorbent but in some cases, it is their byproduct that does. In this context, Eljamal et al. [117] performed a study where copper chloride was added to ZVI and results showed that the removal mechanism occurred as a result of the copper ferrite spinel that was formed on the ZVI particles. It was a challenge to remove phosphate without intoxication because ZVI is prone to that, but this study has reported better removal values compared to ones found in literature [135, 136]. Analysis showed that particles were aggregated in a necklace-like structure; and due to the aerobic conditions, iron got corroded and produced ferric hydroxides, which are known to be good adsorbents of phosphate, that led to complete removal within the first 30 min [87, 137–139].

In a batch experiment, Wang et al. [118] used nano-zero-valent iron coated with pectin for phosphate removal in a highly concentrated aqueous solution and studied its removal efficacy under varied pH, coexisting ions, and ionic strength. The reported results showed the maximum adsorption capacity to be 277.38 mg-P/g, with physical adsorption as the dominant removal mechanism rather than redox reaction. Perassi, Borgnino [140] reported that in the case of a decrease in removal rate of phosphate with increasing ionic strength, the outer sphere complexes are responsible for the process of adsorption, while Liu et al. [141] noted that the inner sphere surface complexes are the dominating complexes for sorption in case of invariable phosphate removal rate with varying ionic strength, which is the case in phosphate removal using pectin-nanoscale zero-valent

iron. By exhibiting larger surface area than nanoscale zero-valent iron, pectin-nanoscale zero-valent iron achieved a higher removal capacity which was mainly affected by pH. It favored an acidic environment since at low pH values pectin-nanoscale zero-valent iron would be corroded to ferrous ions leading to a decrease in the removal of phosphates and inhibiting chemical precipitation [118].

As noted earlier, the products that are formed when combining ZVI with other compounds might result in even stronger adsorbents than both composites when used solely. Zhao et al. [119] activated persulfate by zero-valent iron through an oxidation process resulting in the production of sulfate radicals which are strong oxidizing agents and could degrade phosphates through electron transfer. In this process, ZVI gets transformed to a more efficient coagulant known as ferric iron [142]. Phosphates existed in the solution in many forms with the most dominant being  $H_2PO_4$  [143, 144].

On the other hand, Sleiman et al. [120] investigated the removal abilities of the oxidative products of ZVI and ZVI itself. Various factors were taken into consideration while assessing the removal efficiency such as ionic strength of the solution, presence of various ions as well as aging of ZVI. In this study, adsorption occurred via ZVI or its oxidized products during an aging time of 2–8 h. This is because fresh ZVI does not contain oxidized iron in the form of  $(Fe_3O_4)$  which would incorporate phosphates. An oxide film which exists on the surface of a fresh ZVI would impede the process of adsorption; this film usually consists of goethite and crystalline lepidocrocite.

Zhang et al. [45] reported high removal of phosphates, especially under an oxic-system. This was attributed to the fact that under this system iron can be oxidized and its products can undergo further oxidation ( $Fe^{2+}$ ). Redox reactions increase the solution's pH promoting the formation of  $Fe(OH)_2$  and  $Fe(OH)_3$  which aid in the removal of phosphates via electrostatic interaction and provide more active sites for phosphates to bind to.

The effect of the presence of chloride ions on the corrosion process was studied where controversial results were presented. Reardon [145] stated that an increase in chloride ions led to a decrease in iron corrosion, while on the other hand, Ruangchainikom et al. [146] reported that chlorides promote the formation of rust.

## Mixed metal oxides

With the objective of increasing the efficiency of phosphate removal from aqueous solutions, metal oxides have been synthesized in a mixture of adsorbents. Table 4 presents a list of recent studies conducted on phosphate sorption using adsorbents composed of mixtures of metal oxides. Metals

**Table 4** Research on Phosphate Removal by Mixed Metal Oxides

Zero-Valent iron	Type of Water	pH	Temperature	Dose	Contact time	Equilibrium Isotherm	Adsorption Capacity	Treatment method	Removal efficiency
lanthanum oxide decorated graphene composite [112]	phosphate solution	6.2	Room temperature	2 mg/1 ml	25 min	Langmuir	82.6 mg/g	Batch experiment	100%
Titania-functionalized graphene oxide [149]	simulated wastewater	6	Room temperature	25 mg/25 ml	1440 min	Langmuir	33.1 mg/g	Adsorption experiments	–
nanosized Fe-Al binary oxide [150]	Phosphate solution	4	308 K	0.1 g/50 ml	12 h	Langmuir	16.4 mg/g	Batch experiment	99.86%
nanocrystalline Fe-Al-Mn ternary oxide nanosorbent	Phosphate solution	3	Room temperature	0.1 g/25 ml	16 h	Langmuir	38.46 mg/g	Batch experiment	99.50%
nano-composite containing akaganeite nanorods ( $\beta$ -FeOOH) and graphene oxide sheets (GO) [99]	Phosphate solution	7	30 °C	0.4 g/l	2 h	Langmuir	45.2 mg/g	Batch experiment	–
nanocomposite magnetic particles functionalized with ZnFeZr-adsorbent [151]	spiked secondary wastewater effluent	7	50 °C	860 mg/l	20 min	Freundlich	3333.3 mg/g	Batch experiment	99.80%
Fe–Mn oxide adsorbent [152]	Phosphate solution	7	308 K	0.5 g/200 ml	200 min	Langmuir	18.4 mg/g	Batch experiment	–
nanosized lanthanum hydroxide doped onto magnetic reduced graphene oxide [153]	river and sewage media	5–7	313 K	40 mg/40 ml	10 min	Langmuir	116.28 mg/g	Batch experiment	88%

**Table 4** (continued)

Zero-Valent iron	Type of Water	pH	Temperature	Dose	Contact time	Equilibrium Isotherm	Adsorption Capacity	Treatment method	Removal efficiency
zirconium oxide-based superparamagnetic adsorbents [154]	Phosphate solution	7	–	0.5 g/l	15 min	Langmuir	15.98 mg/g	Adsorption experiments	–
ZnO-Fe <sub>3</sub> O <sub>4</sub> nanocomposite [155]	Phosphate solution	3.1	25 ± 2 °C	1.35 g/l	53.3 min	–	–	Batch experiment	97.60%
La(III) coagulated graphene oxide [156]	Phosphorus stock solution	7	318 K	0.0125 g	20 min	Langmuir	141.38 mg/g	Mechanical Shaker	–
Fe-Ti bimetal oxides on a sulfonated polymer [157]	synthetic feed solution	7.18 ± 0.27	25 °C	300 mg/30 ml 17.5 mg/31.45 ml	24 h 15 min	Langmuir	59 mg/g	batch experiment column experiments	–
Magnetic zirconium-iron oxide nanoparticles [45]	Phosphorus stock solution	1.5	293 ± 2 K	20 g/l	1000 min	Freundlich	21.3 mg/g	Batch experiment	–
CaO–MgO–Al <sub>2</sub> O <sub>3</sub> –SiO <sub>2</sub> [158]	Phosphate solution	–	–	0.5 g/100 ml	–	Langmuir	44.05 mg/g	Batch experiment	–
Fe/Mn oxide composites [159]	Phosphate stock solution	4	Room temperature	0.02 g/20 ml	90 min	Langmuir	26.04 mg/g	Batch experiment	70%
α-Fe <sub>2</sub> O <sub>3</sub> decorated graphene oxide [160]	Phosphate solution	6	298 K	32.5 mg/50 ml	5 min	Langmuir	93.28 mg/g	Batch experiment	–
Mn-Zn-Ti Oxide [161]	Phosphate stock solution	6	Room temperature	0.2 g/l	90 min	Freundlich	151 mg/g	Batch experiment	–
3D Fe <sub>3</sub> O <sub>4</sub> @ZnO nanocubes [162]	Phosphate stock solution Wastewater	7	25 °C	0.03 g/100 ml	10 min	Sips	100.3 mg/g	Batch experiment	96.70%

**Table 4** (continued)

Zero-Valent iron	Type of Water	pH	Temperature	Dose	Contact time	Equilibrium Isotherm	Adsorption Capacity	Treatment method	Removal efficiency
La(III)-coordinated 3-methacryloxyethylpropyl bi-functionalized graphene oxide [113]	Phosphate solution Wastewater	3	25 °C	–	40 min	Langmuir	104.3 mg/g	Batch experiment	–

have shown to possess exclusive advantages over other adsorbents when mixed. In this context, Chen et al. [112] developed a three-dimensional adsorbent made of lanthanum oxide and graphene nanocomposite which exhibited a phosphate selective adsorption property because it is not influenced by various anionic species in water. The composite works well at pH (4–7) because the composite is negatively charged whereas the major phosphate species is not resulting in an ionic attraction forming an acanthus precipitate, making it suitable for large-scale application because natural wastewater pH is generally low [10, 147].

Zheng et al. [148] reported highly efficient phosphate removal from effluents using recoverable  $\text{La}(\text{OH})_3$ , with the pH value of the effluent played the most important role in reaching higher efficiencies of 96 percent removal of phosphate at pH 4–6.

One element within a large mixture might induce a substantial difference in the efficiency of removal. This was demonstrated by Fang et al. [154] who prepared two core/shell zirconium oxide-based superparamagnetic adsorbents where one contained silicon and the other iron ( $\text{ZrO}_2@ \text{SiO}_2@ \text{Fe}_3\text{O}_4$  and  $\text{ZrO}_2@ \text{Fe}_3\text{O}_4$ ). The nanocomposite containing Fe had much higher selectivity, chemical and magnetic stability when compared to the composite containing Si and the removal occurred by forming Zr-O-phosphate inner-sphere complexation.

Chon et al. [159] addressed the frequently reported advantages provided by multifunctional adsorbents in removing multiple contaminants from water environments. Based on this premise, they developed four different magnetic Fe/Mn oxide composites to be applied for the removal of Zn and  $\text{PO}_4$ . According to the reported study, they synthesized the composite by a two-step precipitation of  $\text{Fe}^{2+}$  and  $\text{Mn}^{2+}$  in sequential order whereby the highest removal capacity of phosphates was attained since it holds the highest point of zero charge upon which phosphate removal is favored, as reported in the literature. Fitting the pseudo-second-order reaction rate model, the main mechanism of removal was

suggested to be chemical bonding between the adsorbent and the targeted ions; however, the composite was successful in removing 70% of phosphate ions. Awual et al. [163] and Cui et al. [164] both reported that metal oxides surface charges can be altered by hydrogen or heteroatom bonding reactions. Hence, based on the zeta potential and pH effects, specific sorption could have occurred along with electrostatic attraction as sorption mechanisms.

Bai et al. [160] were successful in engineering a 3D  $\alpha\text{-Fe}_2\text{O}_3$  decorated graphene oxide that was able to sustain removal efficiency on a wide range of pH and remove phosphates rapidly from phosphate polluted water. By reaching equilibrium in 5 min, this renders  $\alpha\text{-Fe}_2\text{O}_3$  decorated graphene oxide the fastest metal oxide to achieve phosphate removal. Ion exchange and electrostatic attraction were the dominant mechanisms of adsorption according to kinetic reaction studies.

On the other hand, a composite of three metal oxides (Mn-Zn-Ti) has been fabricated for the removal of phosphate from aqueous solutions [161]. Adsorption of phosphates on Mn-Zn-Ti oxides composites occurred after the protonation of the hydroxyl group present on the surface of this composite below the point of zero charge (pH = 6.2). After that phosphate anions replaced these hydroxyl groups leading to the formation of monodentate and bidentate complexes. Metal oxides can last for five cycles of adsorption and desorption, and this nanocomposite was also successful in phosphate removal from industrial effluents indicating its practicality at a commercial level.

Ultrafast sorption of phosphate ions (94.8% phosphate capturing in 5 min) was attained using 3D  $\text{Fe}_3\text{O}_4@ \text{ZnO}$  nano-cubes aided by an extra magnet applied at the bottom of the adsorption system creating a weak magnetic field [162]. There are two main causes behind the fast capturing of phosphates, the first being that the endowed Lorentz force by the weak magnetic field pointed phosphate ions to the center of the mixer and secondly the weak magnetic field has triggered electrostatic interactions by exposing the sorbent to

a superior activity. Accordingly, this led to bypassing a rate limiting step and resulted in rapid phosphate sorption [165]. However, the adsorption capacity slightly decreased because of the presence of other anions in the mixture.

La(III)-coordinated 3-methacryloxyethyl-propyl bi-functionalized graphene oxide was prepared to achieve excellent phosphate removal from water [113]. The aforementioned polymer operates optimally under neutral to acidic pH conditions, for adsorption of phosphates [166]. At a pH range of 2–7, the prevalent phosphate form in aqueous solutions is dihydrogen phosphate, when high removal efficiency is reported under these conditions; this indicates the high affinity of La ions to monovalent phosphates anions.

The controlling factor for ligand exchange process is the pH value, when  $\text{pH} < 8$  (point of zero charge), the protonated  $\text{La-OH}_2^+$  is displaced by hydroxyl groups in acidic medium where it can interact with negative charged phosphate ions via electrostatic forces, leading to the uptake of phosphates on the ligand surface. Finally, La(III)-coordinated 3-methacryloxyethyl-propyl bi-functionalized graphene oxide has shown excellent selectivity and good reusability rendering it a good candidate for phosphate removal from wastewater.

Tofik et al. [150] assessed the phosphate sorption capacity of a synthesized Fe–Al binary oxide nano-sorbent, and the experimentation resulted in a high phosphate removal efficiency of approximately 99.8%. The mechanism of adsorption favored lower pH values (99.8% removal efficiency at pH 4), where protonation of metals took place under acidic conditions thus providing more active sites for the uptake of phosphates. Additionally, under similar conditions, the major species of phosphates were determined to be  $\text{H}_2\text{PO}_4^-$ , which is negatively charged and known to have a higher sorption affinity compared to other phosphate species [139, 167]. On the other hand, at higher pH values, the exact opposite occurs, since both the composite and the phosphates are negatively charged; this leads to the repulsion of phosphates ions. Even though this study achieved high removal efficiencies, it remained lower than other values reported in similar studies [168].

The effect of pH variation on the mechanism of phosphate adsorption was also reported by Abebe et al. [169]; the study tested synthesized Nanocrystalline Fe-Al-Mn ternary oxide; as a result, a pH range of 3–7 returned the highest adsorption efficiencies. Similar results were presented by Harijan, Chandra [99] where phosphate groups adsorbed well to the akaganeite nanorods and graphene oxide sheets nanocomposite ( $\beta\text{-FeOOH}$  nanorods/GO) at lower pH; however, under highly acidic conditions ( $\text{pH} < 3$ ) the dissociation of the nanocomposite lead to a decrease in adsorption efficiency.

Du et al. [152] and Szlachta, Chubar [170] claimed that the removal of phosphorus by Fe–Mn oxide was highly dependent on the pH level as it dictates whether phosphate removal occurs

via the replacement of OH groups or not. Whereas Drenkova-Tuhtan et al. [151] and Drenkova-Tuhtan et al. [171] suggested otherwise, where the synthesized adsorbent ( $\text{ZnFeZr-Fe}_3\text{O}_4/\text{SiO}_2$  particles) worked well under a wider range of pH. While the mechanism of action was still being investigated, yet it was suggested that the mechanism possibly was that of complexation of inner-sphere surface, outer-sphere surface and hydrogen bonding.

Several studies reported good adsorption under acidic conditions, which is attributed to the protonation of the adsorbent surface. Sakulpaisan et al. [149] functionalized titania with graphene oxide which led to a synergistic effect especially under acidic solutions, where the surface of the composite is positively charged, and the phosphate charge ( $\text{H}_3\text{PO}_4$  and  $\text{H}_2\text{PO}_4^-$ ) is negative thus leading to adsorption by electrostatic attraction. Similarly, [153] utilized lanthanum hydroxide doped onto magnetic reduced oxide as an adsorbent where electrostatic interaction was the key criterion responsible in the adsorption process, which occurred between negatively charged  $\text{H}_2\text{PO}_4^-$  and the positively charged composite. Analysis also showed a decrease in sorption at pH values above 8 due to the electrostatic competition between hydroxides and phosphates.

Similar results were reported on using  $\text{ZnO-Fe}_3\text{O}_4$  composite where the highest adsorption occurred at pH 3.1. To enhance this outcome, Park et al. [157] used polymer beads coated with mixed metal oxides with titanium being one. It was revealed that  $\text{Ti}^{+4}$  attracted negatively charged phosphates to the surface where at acidic pH the composite had high selectivity to phosphates, which contradicts studies reported in the literature [171, 172]. In addition, a study by Zhang et al. [45] provided more evidence on how low pH (3–7) promotes higher phosphate removal. Upon using magnetic zirconium oxide as the adsorbent, phosphate was removed via inner-sphere complexing mechanism at low pH and decreased with increasing pH due to the increase in hydroxyl groups that compete with phosphates. Zirconium oxide played a major role in the removal of phosphates as was also reported by Long et al. [173].

Contradictory to the studies cited above, a study was conducted by Chen et al. [156] to assess the removal efficiency of lanthanum coagulated graphene oxide as an adsorbent. Analysis of this study showed that positively charged lanthanum acts as the binding force and coagulates phosphates to graphene oxide which works efficiently under neutral to alkaline pH and with reduced efficiency under acidic conditions.

## Chitosan experimental setup and main mechanism of removal

Nanotechnological literature showcases the ascendancy of chitosan as an adsorbent over other nanomaterials, due to its organic origin, easy biodegradability, fusion abilities, and disincentive properties against a wide range of pollutants including nutrients, bacteria and metals [10, 174, 175]. Table 5 presents recently published studies on phosphate removal from water and wastewater.

Generally, the efficiency of chitosan's disincentive properties is highly dependent on initial dose of the chitosan composite, initial concentration of pollutant, contact time, surface area, ionic concentration, and pH. The presented studies that follow highlight the recently conducted research on the use of chitosan as an adsorbent for the removal of phosphates.

Chitosan has been used as an adsorbent to remove nutrients such as phosphates and nitrates. Work on this process was conducted and reported by Zhao, Feng [40] where chitosan was modified into microspheres which allowed adsorption to occur both chemically and physically as was denoted by the pseudo-second-order kinetic model and Dubinin–Radushkevich isotherm model. At first, adsorption occurred at the surface of the microspheres and eventually diffused through the pores. Analysis showed that the adsorption rate is dependent on pH, contact time, initial solution concentration and adsorbent dosage.

Chitosan could be manipulated into different structures. In doing so, Bozorgpour et al. [176] prepared two different structured adsorbents: Chitosan/Al<sub>2</sub>O<sub>3</sub>/Fe<sub>3</sub>O<sub>4</sub> in the form of a fibrous adsorbent and another in the form of beads, whereby their removal efficiencies were compared. Temperature, contact time, initial concentration of phosphate and the presence of other ions in solution played a role in the adsorption rate, where lower pH values favored higher adsorption while at higher pH the electrostatic interactions were negligible. Pseudo-second-order kinetic model was used to fit the kinetics of adsorption. The adsorption behavior was a result of the protonation of the functional groups in the chitosan (NH<sub>2</sub> and OH). Results finally showed a higher removal potential of the nanofibrous composite compared to the bead composites, which may be justified due to the larger surface area available for adsorption in the nanofibrous composite.

In this context, Kumar, Viswanathan [179] formed amine grafted chitosan beads in order to remediate phosphate in a batch mode experiment, where certain parameters like pH, contact time, co-ions presence and temperature were optimized. The phosphate species that was dominant in the sample was H<sub>2</sub>PO<sub>4</sub><sup>-</sup> where it had high affinity to electrostatically bind to the protonated surface of the sorbent forming a

complex. An additional advantage is that the composite can be regenerated and reused for up to six cycles, giving it an edge over conventional methods.

As noted earlier, chitosan could be manipulated into different structures as well as combined with other compounds. Yazdani et al. [177] performed an experiment to study the abatement ability of a bio-sorbent (chitosan-Zinc (II)) in a batch mode. Adsorption was favored in a pH range of 4–7, since at this range the bio-sorbent surface charge is driven to neutrality or positivity. In addition, the higher the volumes of adsorbent the higher is the removal rate, due to the presence of higher surface areas for the phosphates to encounter; especially that it was revealed that the presence of other ions in the solution had low to no effect on phosphate adsorption.

Selective adsorption is a leading edge method, due to the magnetic properties of chitosan [37, 39]. Zavareh et al. [178] attempted to deploy a chitosan-based magnetic adsorbent, where Cu–chitosan/Fe<sub>3</sub>O<sub>4</sub> was the nanocomposites used which was characterized by having a porous surface with high specific area (Fig. 4). According to the Langmuir isotherm, the developed magnetic adsorbent had higher adsorptive capacity compared to raw chitosan/Fe<sub>3</sub>O<sub>4</sub> composite. Neutral pH values depicted the highest removal rates due to high selectivity for phosphates; this occurs when Cu(II) forms a complex with phosphate.

Because chitosan is an eco-friendly adsorbent, it formed an attractive material for many researchers to experiment on its nutrient removal abilities [187, 188]. To make use of chitosan's properties and those of bentonites, Kumar, Viswanathan [189] combined the two composites into one with the addition of metal ions (Zr<sup>4+</sup>, Fe<sup>3+</sup>, and Ca<sup>2+</sup>). The mechanism of action followed many processes that included ion exchange and electrostatic attraction to the composite while controlling pH, initial phosphate concentration, agitation time and presence of anions. The metals with higher valence ions had a higher tendency to attract phosphate to the composite leading to their removal.

Applying iron oxide to chitosan nanoparticles was performed by Kim et al. [180] to enhance the properties of chitosan by taking advantage of the characteristics of iron. The study showed low sensitivity to pH changes, were removal occurred initially by diffusion through the pores leading to ligand exchange between iron oxide and phosphates, it was reported that phosphates replaced the OH group attached to iron achieving a phosphate removal of 52.3%.

The main experimental configuration utilized when testing for chitosan as an adsorbent is a batch mode process, the reason being to allow enough contact time to achieve maximum phosphate removal [190, 191]. Banu, Meenakshi [181] adopted the same experimental procedure using the composite chitosan grafted quaternized resin. Removal showed to be an exothermic process. Many parameters were controlled because of their impact on adsorption like initial

**Table 5** Research on Phosphate Removal Using Chitosan

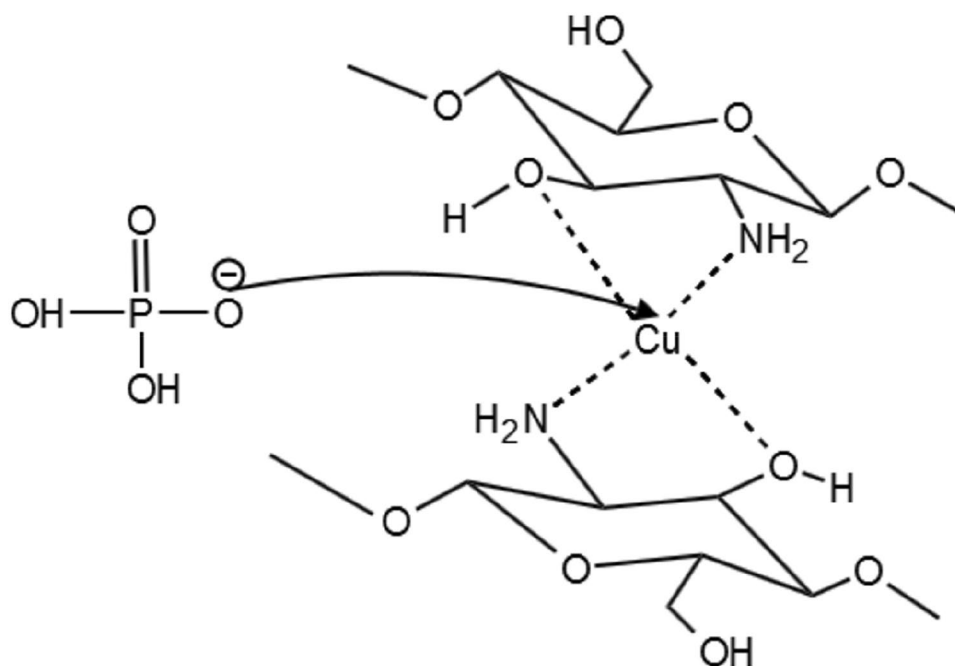
Modified Chitosan	Type of Water	pH	Temperature	Chitosan Dose	Contact time	Equilibrium Isotherm	Adsorption Capacity	Treatment method	Removal Efficiency
modified chitosan microspheres [40]	distilled water	3	303.15 °K	1 g/l	90 min	Langmuir	33.9 mg/g	Batch experiment	
chitosan/Al <sub>2</sub> O <sub>3</sub> /Fe <sub>3</sub> O <sub>4</sub> composite nanofibrous and bead [176]	distilled water	3	20 °C	2%	60 min for nanofibers 120 min for beads	Freundlich for nanofibers Langmuir for beads	151.1 mg/g (nanofibers) 61.9 mg/g (beads)	Batch experiment	
zinc(II)-chitosan complexes [177]	Reverse osmosis water	4	20 °C	0.5 mg/l	180 min	Sips and Freundlich	6.55 mg/g	Batch experiment	97.63% for 1 mg/l of phosphate
Cu-chitosan/Fe <sub>3</sub> O <sub>4</sub> nanocomposite [178]	distilled water	7	Room Temperature	2 g/l	2 h	Langmuir	88 mg/g	Batch experiment	
Zr-Chitosan Bentonite Fe-Chitosan Bentonite Ca-Chitosan Bentonite [179]	Double distilled water	3	323 °K	0.1 g/100 ml	40 min	Freundlich	40.86 mg/g 22.15 mg/g 13.44 mg/g	Batch experiment	
Iron oxide nanoparticle-chitosan [180]	Stream Water	5–9 –7.1	45 °C –	50 g/l 420 g 135 g/l	12 h – 6 min	Redlich–Peterson and Freundlich	0.04 mg/g 0.143 mg/g 0.059 mg/g	Batch experiment Column experiment Field experiment	100% – 52.3%
chitosan quaternized resin [181]	Stock Solution	4–10	303 °K	0.1 g	45 min	Freundlich	181.29 mg/g	Batch experiment	90%
Unicellular cyanobacterium <i>Synechocystis</i> sp. And chitosan [182]	Water from recirculating fish tank	7.5	Room Temperature	20 mg/l	90 min	–	–	Flocculation	>90%



**Table 5** (continued)

Modified Chitosan	Type of Water	pH	Temperature	Chitosan Dose	Contact time	Equilibrium Isotherm	Adsorption Capacity	Treatment method	Removal Efficiency
hydrogel chitosan sorbent ionically cross-linked with sodium citrate and covalently cross-linked with epichlorohydrin [183]	nutrient solution	3		0.2 g	2 h	Langmuir	1.23 mmol/g	Batch experiment	
Tri-ethylene tetramine-functionalized magnetic graphene oxide chitosan composite [45]	Stock Solution	3	298 °K	0.1 g/250 ml	50 min	Langmuir	353.36 mg/g		
Modified carbon nanotubes with chitosan [184]	Ultrapure water	3	293 °K	0.05 g/300 ml	30 min	Freundlich	36.1 ± 0.3 mg/g	Batch experiment	
3-chloro-2-hydroxypropyl trimethylammonium chloride-carboxymethyl chitosan [41]	Distilled water + stock solution	4	–		58 min	–		Jar test	97.80%
amine-functionalized magnetic chitosan composite beads [185]	Stock Solution	varied pH	323 °K	0.1 g/50 ml	40 min	Freundlich	42.95 mg/g	Batch experiment	
lanthanum (III) encapsulated chitosan-montmorillonite composite [186]	Double distilled water	3–7	Ambient Temperature	0.1 g/50 ml	30 min	Freundlich	45 mg/g	Batch experiment	92%

**Fig. 4** Proposed Mechanism of Removal of Phosphate by Cu-chitosan/nano-Iron Oxide [178]



concentration of phosphate, chitosan dosage, pH, presence of anions, temperature, and contact time. The removal mechanism was similar as that of other studies which followed the pattern of electrostatic attraction leading to ion exchange, at which phosphates replaced the  $\text{Cl}^-$  ion located in the quaternary site of the composite. Analysis showed that hydrogen bonds were formed and acted as the removal mechanism. Overall, the experimental results best fitted a pseudo-second-order and Freundlich isotherm models.

Chitosan may potentially be used in combination with living microorganisms to remediate polluted water bodies. In this context, Rojsitthisak et al. [182] attempted to remove phosphate using cyanobacteria in combination with chitosan flocculants. In treating water recirculated from a fish tank, the flocculation efficiency of chitosan was observed while controlling the pH, concentration of chitosan as well as bacterial cells; this resulted in phosphate removal levels of over 90%.

Chitosan has dominance over other nanocomposites because it can be combined with ions covalently and ionically [192–194]. Chitosan was cross-linked ionically with sodium citrate and covalently with epichlorohydrin forming a hydrogel by Józwiak et al. [183]. Compared to other studies, the effects of pH and contact time were studied because of their ascertained impact on sorption efficiency. Nutrients like phosphates were adsorbed physically on the gel's surface because of the amine groups, which could be protonated, i.e., attach to hydrogen ions found in some phosphate species occupying the active sites within the gel's pores. Removal of phosphate species reached 72% thus concluding

that cross-linked chitosan can be a potential applicant to be used in the removal of various nutrients.

As noted in several studies, metals have been combined with chitosan to form functional adsorbents. A study was conducted by Zhang et al. [45] in which they combined magnetic graphene oxide with chitosan. The process was determined to be highly dependent on pH. This can be attributed to the presence of  $-\text{NH}_2$  group on the composite material, and in a matter like that discussed earlier, the phosphates are strongly attracted to the  $-\text{NH}_2$  group at lower pH because of electrostatic interaction. Analysis of the model well-fitted the Langmuir isotherm; this composite has established its functionality in the nanotechnology field because it can be reused for about three cycles.

Studies remain to be limited when it comes to the application of chitosan in combination with carbon nanotubes; thus, a need exists for further investigations in this area [195]. A study was conducted by Huang et al. [184] to functionalize multiwalled carbon nanotubes with chitosan in which 98% removal of phosphates was achieved. The removal was attributed to electrostatic attraction because the adsorbent's surface is positively charged leading to the attraction of phosphate anion; results further show that the reaction fits well the Freundlich isotherm model.

Flocculation is another area where chitosan is being applied. In a study performed by Agbovi, Wilson [41], an amphoteric flocculant (3-chloro-2-hydroxypropyl trimethylammonium chloride onto carboxymethyl chitosan, CMC-CTA) was developed for use in the removal of phosphates from water. Result showed that the removal of phosphorus followed the pseudo-first-order model where the flocculation

process involved neutralization of the charges resulting in the formation of polymer bridges leading to adsorption. The presence of  $\text{Fe}^{+3}$  metal improved the removal of phosphates.

Thagira Banu et al. [186] developed a lanthanum (III) encapsulated chitosan-montmorillonite composite (La-CS-MMT) that effectively removes phosphates, and which has reusability advantages which was maintained at 70% adsorption of phosphates after five cycles of usage. The procedure behind the adsorptions lay in the fact that the La-CS-MMT surface is positively charged with the predominant form of phosphates in the sample being negatively charged ( $\text{H}_2\text{PO}_4^-$ ), by forming hydrogen bonds through electrostatic attraction phosphate is adhered to the surface.

## Conclusion

A comprehensive review of recent studies related to the removal of phosphates from aqueous solutions using adsorption processes was conducted. Different types of adsorbing materials, with emphasis on metal oxides and chitosan and combinations of same, were probed for removal efficiencies and removal mechanisms, leading to their technical feasibility and efficacy for application as viable materials for the removal of phosphates from water and wastewater. Moreover, research gaps were identified in some studies and discussed. The main limitations depicted during the study were related to the lack of modelling studies on the kinetics of the removal mechanisms as applied in the presence of ionic species hindering the removal of the adsorbate.

The evaluated studies, invariably conducted on a bench scale, have shown adequate removal efficiencies of phosphate through the application of different combinations of chitosan and metal oxides, though scaling up of the treatment techniques to the industrial level, on which studies are lacking, might show different results. Moreover, the sustainability of the synthesized sorbents requires further study and evaluation.

Even though several studies have considered applying the synthesized sorbents for the removal of phosphates in the presence of different pollutants, many other studies lack this scenario. The existence of other pollutants may impede the removal efficiencies and thus negatively impact the applicability of such nano-sorbents. Consequently, future studies should take into consideration the typical constituents present in the water to be treated, especially in the case of wastewaters which harbor a vast variety of pollutants.

Additionally, a comprehensive understanding of the mechanisms associated with phosphate removal when utilizing metal oxides and chitosan as nano-sorbents requires the application of universal parametric variations, through varying all the key parameters that have an impact on the process removal efficiency. Based on that, a suitable kinetic

model and proper understanding of the competence of the synthesized sorbent may be attained for most environmental applications.

Phosphate compounds contaminations are on the rise in water bodies and wastewater, and thus, it is critical to develop methods for removal of these compounds. Finding better and more effective sorbents to remove phosphates from water bodies is imperative. From this literature review, we could conclude that both metal oxides and chitosan nano-sorbents showed exceptional potential in the removal of phosphates from water under various conditions. As stated, multiple studies conducted on the removal of phosphates using the material found great success, with removal percentages reaching as high as 99.8 percent in certain batch runs. The major limitation common to most of the surveyed literature is the lack of pilot studies and commercial applications. Almost all the literature report on the removal under controlled experimental conditions.

Without a doubt, given the high demand on the application of chitosan-based materials in removal of phosphates from water and wastewater, the fabrication and development of such adsorbents will continue to evolve. Additionally, future research should focus largely on the development of cheaper alternatives and cleaner technologies based on nanomaterials, and it is critical to prove the application feasibility of such material and should not be limited to controlled experimental conditions. The regeneration and re-use of metal oxides and chitosan-based nano-sorbents should be addressed as well; this is imperative in limiting the waste generated from large- and small-scale applications of these processes. Running batch tests with contaminated wastewater (with phosphates, nitrates, and natural organic matter) allows the assessment of adsorptive selectivity of these processes.

In concluding, it would be reasonable to classify metal oxides and chitosan nano-sorbents and their combinations as promising materials to be applied for the removal of phosphate from aqueous solutions. Nevertheless, the application of these materials at the industrial level calls for further investigations and research to cover the gaps in knowledge related to field applicability, sustainability, cost effectiveness, and environmental/human health impacts.

**Author contributions** All authors contributed to the study conception, design, material preparation, and analysis. More specifically, George M. Ayoub came up with the idea for the article, Assaad Hassan Kassem and Ramez M. Zayyat performed the literature search and data analysis, and George M. Ayoub drafted and critically revised the work.

**Funding** No funding was received to assist with the preparation of this manuscript. The authors have no conflicts of interest to declare that are relevant to the content of this article.

**Availability of data and materials** Not Applicable.

## Declarations

**Competing interests** The authors declare that they have no competing interests.

**Ethical approval** Not applicable.

**Consent to participate** Not applicable.

**Consent for publication** All authors approve this manuscript for publication.

## References

- Silveira MAD, Ribeiro DL, Vieira GM, Demarco NR, d'Arce LPG (2018) Direct and indirect anthropogenic contamination in water sources: evaluation of chromosomal stability and cytotoxicity using the allium cepa test. *Bull Environ Contam Toxicol* 100(2):216–220. <https://doi.org/10.1007/s00128-017-2232-1>
- Monte Egitto L, Medeiros M, Batistuzzo S, Agnez-Lima L (2007) Cytotoxic and genotoxic potential of surface water from the Pitimbu river, Northeastern/RN Brazil. *Genet Mol Biol*. <https://doi.org/10.1590/S1415-47572007000300023>
- Wach T, Kozakiewicz M (2021) Are recent available blended collagen-calcium phosphate better than collagen alone or crystalline calcium phosphate? Radiotextural analysis of a 1-year clinical trial. *Clin Oral Invest* 25(6):3711–3718. <https://doi.org/10.1007/s00784-020-03697-4>
- Gong Y, Zhao D (2013) Physical-chemical processes for phosphorus removal and recovery. *Compr Water Quality Purif* 3:196–222. <https://doi.org/10.1016/B978-0-12-382182-9.00086-4>
- Xu X, Gao B, Jin B, Yue Q (2016) Removal of anionic pollutants from liquids by biomass materials: A review. *J Mol Liq* 215:565–595. <https://doi.org/10.1016/j.molliq.2015.12.101>
- Huang W, Zhang Y, Li D (2017) Adsorptive removal of phosphate from water using mesoporous materials: a review. *J Environ Manage* 193:470–482. <https://doi.org/10.1016/j.jenvman.2017.02.030>
- Lin K (2009) Joint acute toxicity of tributyl phosphate and triphenyl phosphate to *Daphnia magna*. *Environ Chem Lett* 7(4):309–312. <https://doi.org/10.1007/s10311-008-0170-1>
- Eltaweil AS, Omer AM, El-Aqapa HG, Gaber NM, Attia NF, El-Subruiti GM et al (2021) Chitosan based adsorbents for the removal of phosphate and nitrate: a critical review. *Carbohydr Polym* 274:118671. <https://doi.org/10.1016/j.carbpol.2021.118671>
- Laroussi M, Mendis DA, Rosenberg M (2003) Plasma interaction with microbes. *New J Phys* 5:41. <https://doi.org/10.1088/1367-2630/5/1/341>
- Yang K, Yan L-G, Yang Y-M, Yu S-J, Shan R-R, Yu H-Q et al (2014) Adsorptive removal of phosphate by Mg–Al and Zn–Al layered double hydroxides: Kinetics, isotherms and mechanisms. *Sep Purif Technol* 124:36–42. <https://doi.org/10.1016/j.seppur.2013.12.042>
- Yang S, Zhao Y, Chen R, Feng C, Zhang Z, Lei Z et al (2013) A novel tablet porous material developed as adsorbent for phosphate removal and recycling. *J Colloid Interface Sci* 396:197–204. <https://doi.org/10.1016/j.jcis.2012.12.077>
- Huang W, Cao X, Huang D, Liu W, Liu X, Zhang J (2019) Phosphorus characteristics and microbial community in the sediment-water-algal system during algal growth. *Environ Sci Pollut Res* 26(30):31414–31421. <https://doi.org/10.1007/s11356-019-06284-7>
- Zhang C, Wang X, Ma Z, Luan Z, Wang Y, Wang Z et al (2020) Removal of phenolic substances from wastewater by algae. review. *Environ Chem Lett* 18(2):377–392. <https://doi.org/10.1007/s10311-019-00953-2>
- Khalil AME, Eljamal O, Amen TWM, Sugihara Y, Matsunaga N (2017) Optimized nano-scale zero-valent iron supported on treated activated carbon for enhanced nitrate and phosphate removal from water. *Chem Eng J* 309:349–365. <https://doi.org/10.1016/j.cej.2016.10.080>
- Rigueto CVT, Nazari MT, Massuda LÁ, Ostwald BEP, Piccin JS, Dettmer A (2021) Production and environmental applications of gelatin-based composite adsorbents for contaminants removal: a review. *Environ Chem Lett* 19(3):2465–2486. <https://doi.org/10.1007/s10311-021-01184-0>
- Tafu M, Sasakawa N, Murthy HS, Takamatsu S, Manaka A, Irie M et al (2020) Effective removal of fluoride and phosphate pollution using mixtures of dicalcium phosphate dihydrate (DCPD) and Tunisian reservoir sediment containing calcium carbonate. *Euro-Mediterr J Environ Integr* 5(1):1. <https://doi.org/10.1007/s41207-019-0135-8>
- Ayoub GM, Semerjian L (2006) Low cost processes for the removal of phosphates in water and wastewater. *Int J Environ Technol Manage* 6(5):448–465. <https://doi.org/10.1504/ijetm.2006.010477>
- Ayoub GM, Kalinian H, Zayyat R (2019) Efficient phosphate removal from contaminated water using functional raw dolomite powder. *SN Appl Sci* 1(7):802. <https://doi.org/10.1007/s42452-019-0833-5>
- Ayoub GM, Koopman B, Pandya N (2001) Iron and Aluminum Hydroxy (Oxide) coated filter media for low-concentration phosphorus removal. *Water Environ Res* 73(4):478–485. <https://doi.org/10.2175/106143001X139533>
- Ayoub GM, Kalinian H (2006) Removal of low-concentration phosphorus using a fluidized raw dolomite bed. *Water Environ Res* 78(4):353–361. <https://doi.org/10.2175/106143005X90001>
- Zhao F, Yang W, Zeng Z, Li H, Yang X, He Z et al (2012) Nutrient removal efficiency and biomass production of different bioenergy plants in hypereutrophic water. *Biomass Bioenerg* 42:212–218. <https://doi.org/10.1016/j.biombioe.2012.04.003>
- Jutidamrongphan W, Park KY, Dockko S, Choi JW, Lee SH (2012) High removal of phosphate from wastewater using silica sulfate. *Environ Chem Lett* 10(1):21–28. <https://doi.org/10.1007/s10311-011-0323-5>
- Liu R, Chi L, Wang X, Sui Y, Wang Y, Arandiyani H (2018) Review of metal (hydr)oxide and other adsorptive materials for phosphate removal from water. *J Environ Chem Eng* 6(4):5269–5286. <https://doi.org/10.1016/j.jece.2018.08.008>
- Ma Z, Li Q, Yue Q, Gao B, Li W, Xu X et al (2011) Adsorption removal of ammonium and phosphate from water by fertilizer controlled release agent prepared from wheat straw. *Chem Eng J* 171(3):1209–1217. <https://doi.org/10.1016/j.cej.2011.05.027>
- Prashantha Kumar TKM, Mandlimath TR, Sangeetha P, Revathi SK, Ashok Kumar SK (2018) Nanoscale materials as sorbents for nitrate and phosphate removal from water. *Environ Chem Lett* 16(2):389–400. <https://doi.org/10.1007/s10311-017-0682-7>
- Ouasfi N, Bouzekri S, Zbair M, Ait Ahsaine H, Bakkas S, Bensitel M et al (2019) Carbonaceous material prepared by ultrasonic assisted pyrolysis from algae (*Bifurcaria bifurcata*): Response surface modeling of aspirin removal. *Surf Interfaces* 14:61–71. <https://doi.org/10.1016/j.surf.2018.11.008>
- Sanad MF, Puente Santiago AR, Tolba SA, Ahsan MA, Fernandez-Delgado O, Shawky Adly M et al (2021) Co–Cu Bimetallic Metal Organic Framework Catalyst Outperforms

- the Pt/C Benchmark for Oxygen Reduction. *J Am Chem Soc* 143(10):4064–4073. <https://doi.org/10.1021/jacs.1c01096>
28. Xu C, Puente-Santiago AR, Rodríguez-Padrón D, Muñoz-Batista MJ, Ahsan MA, Noveron JC et al (2021) Nature-inspired hierarchical materials for sensing and energy storage applications. *Chem Soc Rev* 50(8):4856–4871. <https://doi.org/10.1039/C8CS00652K>
  29. Dominguez N, Torres B, Barrera LA, Rincon JE, Lin Y, Chianelli RR et al (2018) Bimetallic CoMoS composite anchored to biocarbon fibers as a high-capacity anode for Li-Ion batteries. *ACS Omega* 3(8):10243–10249. <https://doi.org/10.1021/acsomega.8b00654>
  30. Ahsan MA, Imam MA, Puente Santiago AR, Rodriguez A, Alvarado-Tenorio B, Bernal R et al (2020) Spent tea leaves templated synthesis of highly active and durable cobalt-based trifunctional versatile electrocatalysts for hydrogen and oxygen evolution and oxygen reduction reactions. *Green Chem* 22(20):6967–6980. <https://doi.org/10.1039/DOG02155E>
  31. Ahsan MA, He T, Eid K, Abdullah AM, Curry ML, Du A et al (2021) Tuning the intermolecular electron transfer of low-dimensional and metal-free BCN/C60 electrocatalysts via interfacial defects for efficient hydrogen and oxygen electrochemistry. *J Am Chem Soc* 143(2):1203–1215. <https://doi.org/10.1021/jacs.0c12386>
  32. Ahsan MA, Puente Santiago AR, Sanad MF, Mark Weller J, Fernandez-Delgado O, Barrera LA et al (2021) Tissue paper-derived porous carbon encapsulated transition metal nanoparticles as advanced non-precious catalysts: carbon-shell influence on the electrocatalytic behaviour. *J Colloid Interface Sci* 581:905–918. <https://doi.org/10.1016/j.jcis.2020.08.012>
  33. Ahsan MA, Puente Santiago AR, Rodriguez A, Maturano-Rojas V, Alvarado-Tenorio B, Bernal R et al (2020) Biomass-derived ultrathin carbon-shell coated iron nanoparticles as high-performance tri-functional HER, ORR and Fenton-like catalysts. *J Clean Prod* 275:124141. <https://doi.org/10.1016/j.jclepro.2020.124141>
  34. Velusamy K, Periyasamy S, Kumar PS, Vo D-VN, Sindhu J, Sneha D et al (2021) Advanced techniques to remove phosphates and nitrates from waters: a review. *Environ Chem Lett*. <https://doi.org/10.1007/s10311-021-01239-2>
  35. Zbair M, Anfar Z, Ahsaine HA (2019) Reusable bentonite clay: modelling and optimization of hazardous lead and p-nitrophenol adsorption using a response surface methodology approach. *RSC Adv* 9(10):5756–5769. <https://doi.org/10.1039/C9RA00079H>
  36. Anfar Z, Zbair M, Ait Ahsiane H, Jada A, El Alem N (2020) Microwave assisted green synthesis of Fe2O3/biochar for ultrasonic removal of nonsteroidal anti-inflammatory pharmaceuticals. *RSC Adv* 10(19):11371–11380. <https://doi.org/10.1039/D0RA00617C>
  37. Lichtfouse E, Morin-Crini N, Fourmentin M, Zemmouri H, do Carmo Nascimento IO, Queiroz LM et al (2019) Chitosan for direct bioflocculation of wastewater. *Environ Chem Lett* 17(4):1603–1621. <https://doi.org/10.1007/s10311-019-00900-1>
  38. Zare EN, Mudhoo A, Khan MA, Otero M, Bundhoo ZMA, Navarathna C et al (2021) Water decontamination using bio-based, chemically functionalized, doped, and ionic liquid-enhanced adsorbents: review. *Environ Chem Lett*. <https://doi.org/10.1007/s10311-021-01207-w>
  39. Crini G (2019) Historical review on chitin and chitosan biopolymers. *Environ Chem Lett* 17(4):1623–1643. <https://doi.org/10.1007/s10311-019-00901-0>
  40. Zhao T, Feng T (2016) Application of modified chitosan microspheres for nitrate and phosphate adsorption from aqueous solution. *RSC Adv* 6(93):90878–90886. <https://doi.org/10.1039/C6RA17474D>
  41. Agbovi HK, Wilson LD (2018) Design of amphoteric chitosan flocculants for phosphate and turbidity removal in wastewater. *Carbohydr Polym* 189:360–370. <https://doi.org/10.1016/j.carbpol.2018.02.024>
  42. Xu H, Hu J, Ren X, Li G (2016) Macroscopic and microscopic insight into the mutual effects of europium(iii) and phosphate on their interaction with graphene oxide. *RSC Adv* 6(88):85046–85057. <https://doi.org/10.1039/C6RA18629G>
  43. Ahmed S, Guo Y, Huang R, Li D, Tang P, Feng Y (2017) Hexamethylene tetramine-assisted hydrothermal synthesis of porous magnesium oxide for high-efficiency removal of phosphate in aqueous solution. *J Environ Chem Eng* 5(5):4649–4655. <https://doi.org/10.1016/j.jece.2017.09.006>
  44. Chen D, Gao B, Wang H, Yang K (2016) Effective removal of high concentration of phosphate by starch-stabilized nanoscale zerovalent iron (SNZVI). *J Taiwan Inst Chem Eng* 61:181–187. <https://doi.org/10.1016/j.jtice.2015.12.007>
  45. Zhang C, Li Y, Wang F, Yu Z, Wei J, Yang Z et al (2017) Performance of magnetic zirconium-iron oxide nanoparticle in the removal of phosphate from aqueous solution. *Appl Surf Sci* 396:1783–1792. <https://doi.org/10.1016/j.apsusc.2016.11.214>
  46. Triantafyllidis KS, Peleka EN, Komvokis VG, Mavros PP (2010) Iron-modified hydrotalcite-like materials as highly efficient phosphate sorbents. *J Colloid Interface Sci* 342(2):427–436. <https://doi.org/10.1016/j.jcis.2009.10.063>
  47. Choe S, Liljestrand HM, Khim J (2004) Nitrate reduction by zero-valent iron under different pH regimes. *Appl Geochem* 19(3):335–342. <https://doi.org/10.1016/j.apgeochem.2003.08.001>
  48. Lee K, Jutidamrongphan W, Lee S, Park KY (2017) Adsorption kinetics and isotherms of phosphate and its removal from wastewater using mesoporous titanium oxide. *Membrane Water Treatment* 8:161–169. <https://doi.org/10.12989/mwt.2017.8.2.161>
  49. Rittmann BE, Mayer B, Westerhoff P, Edwards M (2011) Capturing the lost phosphorus. *Chemosphere* 84(6):846–853. <https://doi.org/10.1016/j.chemosphere.2011.02.001>
  50. Nair AT, Ahammed MM (2015) Water treatment sludge for phosphate removal from the effluent of UASB reactor treating municipal wastewater. *Process Saf Environ Prot* 94:105–112. <https://doi.org/10.1016/j.psep.2015.01.004>
  51. Johir MAH, Pradhan M, Loganathan P, Kandasamy J, Vigneshwaran S (2016) Phosphate adsorption from wastewater using zirconium (IV) hydroxide: Kinetics, thermodynamics and membrane filtration adsorption hybrid system studies. *J Environ Manage* 167:167–174. <https://doi.org/10.1016/j.jenvman.2015.11.048>
  52. Yadav D, Kumar P, Kapur M, Mondal MK (2019) Phosphate removal from aqueous solutions by nano-alumina for the effective remediation of eutrophication. *Environ Prog Sustain Energy* 38(s1):S77–S85. <https://doi.org/10.1002/ep.12920>
  53. Kumar PS, Suganya S, Srinivas S, Priyadarshini S, Karthika M, Karishma Sri R et al (2019) Treatment of fluoride-contaminated water. review. *Environ Chem Lett* 17(4):1707–1726. <https://doi.org/10.1007/s10311-019-00906-9>
  54. Mor S, Chhoden K, Negi P, Ravindra K (2017) Utilization of nano-alumina and activated charcoal for phosphate removal from wastewater. *Environ Nanotechnol Monit Manage* 7:15–23. <https://doi.org/10.1016/j.enmm.2016.11.006>
  55. Shojaeipoor F, Elhamifar D, Moshkelgosha R, Masoumia B (2016) Removal of Pb(II) and Co(II) ions from aqueous solution and industrial wastewater using ILNO-NH2: Kinetic, isotherm and thermodynamic studies. *J Taiwan Inst Chem Eng* 67:166–173. <https://doi.org/10.1016/j.jtice.2016.07.008>
  56. Madhura L, Singh S, Kanchi S, Sabela M, Bisetty K, Inamuddin (2019) Nanotechnology-based water quality management for

- wastewater treatment. *Environ Chem Lett* 17(1):65–121. <https://doi.org/10.1007/s10311-018-0778-8>
57. Cervantes-Avilés P, Cuevas-Rodríguez G (2017) Changes in nutrient removal and flocs characteristics generated by presence of ZnO nanoparticles in activated sludge process. *Chemosphere* 182:672–680. <https://doi.org/10.1016/j.chemosphere.2017.05.074>
  58. Tan M, Qiu G, Ting Y-P (2015) Effects of ZnO nanoparticles on wastewater treatment and their removal behavior in a membrane bioreactor. *Biores Technol* 185:125–133. <https://doi.org/10.1016/j.biortech.2015.02.094>
  59. Lv J, Zhang S, Luo L, Han W, Zhang J, Yang K et al (2012) Dissolution and microstructural transformation of ZnO nanoparticles under the influence of phosphate. *Environ Sci Technol* 46(13):7215–7221. <https://doi.org/10.1021/es301027a>
  60. Anegawa R, Agario A, Shiomi H (2018) Phosphorus removal characteristics of layered zinc hydroxide synthesized from zinc hydroxide sulfate. *J Soc Mater Sci Jpn* 67(6):593–597. <https://doi.org/10.2472/jsms.67.593>
  61. Manzo S, Miglietta ML, Rametta G, Buono S, Di Francia G (2013) Toxic effects of ZnO nanoparticles towards marine algae *Dunaliella tertiolecta*. *Sci Total Environ* 445–446:371–376. <https://doi.org/10.1016/j.scitotenv.2012.12.051>
  62. Odzak N, Kistler D, Behra R, Sigg L (2014) Dissolution of metal and metal oxide nanoparticles in aqueous media. *Environ Pollut* 191:132–138. <https://doi.org/10.1016/j.envpol.2014.04.010>
  63. Suman TY, Radhika Rajasree SR, Kirubakaran R (2015) Evaluation of zinc oxide nanoparticles toxicity on marine algae *Chlorella vulgaris* through flow cytometric, cytotoxicity and oxidative stress analysis. *Ecotoxicol Environ Saf* 113:23–30. <https://doi.org/10.1016/j.ecoenv.2014.11.015>
  64. Miller RJ, Lenihan HS, Muller EB, Tseng N, Hanna SK, Keller AA (2010) Impacts of metal oxide nanoparticles on marine phytoplankton. *Environ Sci Technol* 44(19):7329–7334. <https://doi.org/10.1021/es100247x>
  65. Li M, Zhu L, Lin D (2011) Toxicity of ZnO nanoparticles to *Escherichia coli*: mechanism and the influence of medium components. *Environ Sci Technol* 45(5):1977–1983. <https://doi.org/10.1021/es102624t>
  66. Nurdogan Y, Oswald WJ (1995) Enhanced nutrient removal in high-rate ponds. *Water Sci Technol* 31(12):33–43. [https://doi.org/10.1016/0273-1223\(95\)00490-E](https://doi.org/10.1016/0273-1223(95)00490-E)
  67. Hashimoto K, Irie H, Fujishima A (2005) TiO<sub>2</sub> photocatalysis: a historical overview and future prospects. *Jpn J Appl Phys* 44:8269–8285. <https://doi.org/10.1143/JJAP.44.8269>
  68. Wada K, Nishikawa M, Kishimoto N (2011) Control approach to non-biodegradable organic matter in roadway runoff. *Water Pract Technol*. <https://doi.org/10.2166/wpt.2011.007>
  69. Fujishima A, Zhang X, Tryk D (2007) Heterogeneous photocatalysis: from water photolysis to applications in environmental cleanup. *Int J Hydrogen Energy* 32:2664–2672. <https://doi.org/10.1016/j.ijhydene.2006.09.009>
  70. Urano K, Tachikawa H (1991) Process development for removal and recovery of phosphorus from wastewater by a new adsorbent. II. Adsorption rates and breakthrough curves. *Ind Eng Chem Res* 30(8):1897–1899. <https://doi.org/10.1021/ie00056a033>
  71. Rad S, Shamsudin S, Taha MR, Shahid S (2015) Tropical stormwater nutrient degradation using nano-TiO<sub>2</sub> in photocatalytic reactor detention pond. *Water Sci Technol* 73(2):405–413. <https://doi.org/10.2166/wst.2015.465>
  72. Wang N, Feng J, Chen J, Wang J, Yan W (2017) Adsorption mechanism of phosphate by polyaniline/TiO<sub>2</sub> composite from wastewater. *Chem Eng J* 316:33–40. <https://doi.org/10.1016/j.cej.2017.01.066>
  73. Wang T, Jin X, Chen Z, Megharaj M, Naidu R (2014) Green synthesis of Fe nanoparticles using eucalyptus leaf extracts for treatment of eutrophic wastewater. *Sci Total Environ* 466–467:210–213. <https://doi.org/10.1016/j.scitotenv.2013.07.022>
  74. Wang T, Lin J, Chen Z, Megharaj M, Naidu R (2014) Green synthesized iron nanoparticles by green tea and eucalyptus leaves extracts used for removal of nitrate in aqueous solution. *J Clean Prod* 83:413–419. <https://doi.org/10.1016/j.jclepro.2014.07.006>
  75. Zhuang Z, Huang L, Wang F, Chen Z (2015) Effects of cyclodextrin on the morphology and reactivity of iron-based nanoparticles using Eucalyptus leaf extract. *Ind Crops Prod* 69:308–313. <https://doi.org/10.1016/j.indcrop.2015.02.027>
  76. Cao D, Jin X, Gan L, Wang T, Chen Z (2016) Removal of phosphate using iron oxide nanoparticles synthesized by eucalyptus leaf extract in the presence of CTAB surfactant. *Chemosphere* 159:23–31. <https://doi.org/10.1016/j.chemosphere.2016.05.080>
  77. Kralchevska RP, Prucek R, Kolařík J, Tuček J, Machala L, Filip J et al (2016) Remarkable efficiency of phosphate removal: Ferrate(VI)-induced in situ sorption on core-shell nanoparticles. *Water Res* 103:83–91. <https://doi.org/10.1016/j.watres.2016.07.021>
  78. Lai L, Xie Q, Chi L, Gu W, Wu D (2016) Adsorption of phosphate from water by easily separable Fe<sub>3</sub>O<sub>4</sub>@SiO<sub>2</sub> core/shell magnetic nanoparticles functionalized with hydrous lanthanum oxide. *J Colloid Interface Sci* 465:76–82. <https://doi.org/10.1016/j.jcis.2015.11.043>
  79. Lalley J, Han C, Li X, Dionysiou DD, Nadagouda MN (2016) Phosphate adsorption using modified iron oxide-based sorbents in lake water: Kinetics, equilibrium, and column tests. *Chem Eng J* 284:1386–1396. <https://doi.org/10.1016/j.cej.2015.08.114>
  80. You X, Farran A, Guaya D, Valderrama C, Soldatov V, Cortina JL (2016) Phosphate removal from aqueous solutions using a hybrid fibrous exchanger containing hydrated ferric oxide nanoparticles. *J Environ Chem Eng* 4(1):388–397. <https://doi.org/10.1016/j.jece.2015.11.032>
  81. You X, Valderrama C, Soldatov V, Cortina JL (2018) Phosphate recovery from treated municipal wastewater using hybrid anion exchangers containing hydrated ferric oxide nanoparticles. *J Chem Technol Biotechnol* 93(2):358–364. <https://doi.org/10.1002/jctb.5361>
  82. Gan L, Lu Z, Cao D, Chen Z (2018) Effects of cetyltrimethylammonium bromide on the morphology of green synthesized Fe<sub>3</sub>O<sub>4</sub> nanoparticles used to remove phosphate. *Mater Sci Eng, C* 82:41–45. <https://doi.org/10.1016/j.msec.2017.08.073>
  83. Goodwill JE, Jiang Y, Reckhow DA, Gikonyo J, Tobiason JE (2015) Characterization of particles from ferrate preoxidation. *Environ Sci Technol* 49(8):4955–4962. <https://doi.org/10.1021/acs.est.5b00225>
  84. Wilfert P, Kumar PS, Korving L, Witkamp G-J, van Loosdrecht MCM (2015) The relevance of phosphorus and iron chemistry to the recovery of phosphorus from wastewater: a Review. *Environ Sci Technol* 49(16):9400–9414. <https://doi.org/10.1021/acs.est.5b00150>
  85. Sperlich A, Werner A, Genz A, Amy G, Worch E, Jekel M (2005) Breakthrough behavior of granular ferric hydroxide (GFH) fixed-bed adsorption filters: modeling and experimental approaches. *Water Res* 39(6):1190–1198. <https://doi.org/10.1016/j.watres.2004.12.032>
  86. Kanematsu M, Young T, Fukushi K, Sverjensky D, Green P, Darby J (2011) Quantification of the effects of organic and carbonate buffers on arsenate and phosphate adsorption on a goethite-based granular porous adsorbent. *Environ Sci Technol* 45:561–568. <https://doi.org/10.1021/es1026745>
  87. Chitrakar R, Tezuka S, Sonoda A, Sakane K, Ooi K, Hirotsu T (2006) Phosphate adsorption on synthetic goethite and

- akaganeite. *J Colloid Interface Sci* 298(2):602–608. <https://doi.org/10.1016/j.jcis.2005.12.054>
88. Sleiman N, Deluchat V, Wazne M, Courtin A, Saad Z, Kazpard V et al (2016) Role of iron oxidation byproducts in the removal of phosphate from aqueous solution. *RSC Adv* 6(2):1627–1636. <https://doi.org/10.1039/C5RA22444F>
  89. Fang C, Zhang T, Li P, Jiang R-F, Wang Y (2014) Application of magnesium modified corn biochar for phosphorus removal and recovery from swine wastewater. *Int J Environ Res Public Health* 11:9217–9237. <https://doi.org/10.3390/ijerph110909217>
  90. Jung K-W, Ahn K-H (2016) Fabrication of porosity-enhanced MgO/biochar for removal of phosphate from aqueous solution: application of a novel combined electrochemical modification method. *Biores Technol* 200:1029–1032. <https://doi.org/10.1016/j.biortech.2015.10.008>
  91. Xia P, Wang X, Wang X, Song J, Wang H, Zhang J et al (2016) Struvite crystallization combined adsorption of phosphate and ammonium from aqueous solutions by mesoporous MgO loaded diatomite. *Colloids Surf, A* 506:220–227. <https://doi.org/10.1016/j.colsurfa.2016.05.101>
  92. Li R, Wang JJ, Zhou B, Zhang Z, Liu S, Lei S et al (2017) Simultaneous capture removal of phosphate, ammonium and organic substances by MgO impregnated biochar and its potential use in swine wastewater treatment. *J Clean Prod* 147:96–107. <https://doi.org/10.1016/j.jclepro.2017.01.069>
  93. Ahmed S, Guo Y, Li D, Tang P, Feng Y (2018) Superb removal capacity of hierarchically porous magnesium oxide for phosphate and methyl orange. *Environ Sci Pollut Res* 25(25):24907–24916. <https://doi.org/10.1007/s11356-018-2565-2>
  94. Hermassi M, Dosta J, Valderrama C, Licon E, Moreno N, Querol X et al (2018) Simultaneous ammonium and phosphate recovery and stabilization from urban sewage sludge anaerobic digestates using reactive sorbents. *Sci Total Environ* 630:781–789. <https://doi.org/10.1016/j.scitotenv.2018.02.243>
  95. Ma G, Salahub S, Montemagno C, Abraham S (2018) Highly active magnesium oxide nano materials for the removal of arsenates and phosphates from aqueous solutions. *Nano-Struct Nano-Objects* 13:74–81. <https://doi.org/10.1016/j.nanoso.2017.11.006>
  96. Stratful I, Scrimshaw MD, Lester JN (2001) Conditions influencing the precipitation of magnesium ammonium phosphate. *Water Res* 35(17):4191–4199. [https://doi.org/10.1016/S0043-1354\(01\)00143-9](https://doi.org/10.1016/S0043-1354(01)00143-9)
  97. Karageorgiou K, Paschalis M, Anastassakis GN (2007) Removal of phosphate species from solution by adsorption onto calcite used as natural adsorbent. *J Hazard Mater* 139(3):447–452. <https://doi.org/10.1016/j.jhazmat.2006.02.038>
  98. Yan L-g, Yang K, Shan R-r, Yan T, Wei J, Yu S-j et al (2015) Kinetic, isotherm and thermodynamic investigations of phosphate adsorption onto core-shell Fe<sub>3</sub>O<sub>4</sub>@LDHs composites with easy magnetic separation assistance. *J Colloid Interface Sci* 448:508–516. <https://doi.org/10.1016/j.jcis.2015.02.048>
  99. Harijan DKL, Chandra V (2017) Akaganeite nanorods decorated graphene oxide sheets for removal and recovery of aqueous phosphate. *J Water Process Eng* 19:120–125. <https://doi.org/10.1016/j.jwpe.2017.07.019>
  100. Fawzy S, Osman AI, Yang H, Doran J, Rooney DW (2021) Industrial biochar systems for atmospheric carbon removal: a review. *Environ Chem Lett*. <https://doi.org/10.1007/s10311-021-01210-1>
  101. Patra BR, Mukherjee A, Nanda S, Dalai AK (2021) Biochar production, activation and adsorptive applications: a review. *Environ Chem Lett* 19(3):2237–2259. <https://doi.org/10.1007/s10311-020-01165-9>
  102. Huang H, Zhang P, Zhang Z, Liu J, Xiao J, Gao F (2016) Simultaneous removal of ammonia nitrogen and recovery of phosphate from swine wastewater by struvite electrochemical precipitation and recycling technology. *J Clean Prod* 127:302–310. <https://doi.org/10.1016/j.jclepro.2016.04.002>
  103. Wang H, Zhang P, Liu J (2017) Triethylene tetramine functionalized magnetic graphene oxide chitosan composite with superior capacity for the removal of phosphate. *J Chem Eng Data* 62(10):3341–3352. <https://doi.org/10.1021/acs.jced.7b00417>
  104. Post JE (1999) Manganese oxide minerals: crystal structures and economic and environmental significance. *Proc Natl Acad Sci* 96(7):3447. <https://doi.org/10.1073/pnas.96.7.3447>
  105. Adani F, Tambone F (2005) Long-term effect of sewage sludge application on soil humic acids. *Chemosphere* 60(9):1214–1221. <https://doi.org/10.1016/j.chemosphere.2005.02.031>
  106. Perreault F, Fonseca de Faria A, Elimelech M (2015) Environmental applications of graphene-based nanomaterials. *Chem Soc Rev* 44(16):5861–5896. <https://doi.org/10.1039/C5CS00021A>
  107. Zhao J, Wang Z, White JC, Xing B (2014) Graphene in the aquatic environment: adsorption, dispersion, toxicity and transformation. *Environ Sci Technol* 48(17):9995–10009. <https://doi.org/10.1021/es5022679>
  108. Madima N, Mishra SB, Inamuddin I, Mishra AK (2020) Carbon-based nanomaterials for remediation of organic and inorganic pollutants from wastewater. A review. *Environ Chem Lett* 18(4):1169–1191. <https://doi.org/10.1007/s10311-020-01001-0>
  109. Zhao G, Jiang L, He Y, Li J, Dong H, Wang X et al (2011) Sulfonated graphene for persistent aromatic pollutant management. *Adv Mater* 23(34):3959–3963. <https://doi.org/10.1002/adma.201101007>
  110. Huang G, Guo H, Zhao J, Liu Y, Xing B (2016) Effect of co-existing kaolinite and goethite on the aggregation of graphene oxide in the aquatic environment. *Water Res* 102:313–320. <https://doi.org/10.1016/j.watres.2016.06.050>
  111. Peng X, Mo S, Li R, Li J, Tian C, Liu W et al (2021) Effective removal of the rare earth element dysprosium from wastewater with polyurethane sponge-supported graphene oxide–titanium phosphate. *Environ Chem Lett* 19(1):719–728. <https://doi.org/10.1007/s10311-020-01073-y>
  112. Chen M, Huo C, Li Y, Wang J (2016) Selective adsorption and efficient removal of phosphate from aqueous medium with graphene-lanthanum composite. *ACS Sustain Chem Eng* 4(3):1296–1302. <https://doi.org/10.1021/acssuschemeng.5b01324>
  113. Liu Z, Wu W, Liu Y, Hu X (2018) Preparation of surface anion imprinted polymer by developing a La(III)-coordinated 3-methacryloxyethyl-propyl bi-functionalized graphene oxide for phosphate removal. *J Taiwan Inst Chem Eng* 85:282–290. <https://doi.org/10.1016/j.jtice.2018.02.001>
  114. Arancibia-Miranda N, Baltazar SE, García A, Romero AH, Rubio MA, Altbir D (2014) Lead removal by nano-scale zero valent iron: Surface analysis and pH effect. *Mater Res Bull* 59:341–348. <https://doi.org/10.1016/j.materresbull.2014.07.045>
  115. Jiang Z, Lv L, Zhang W, Du Q, Pan B, Yang L et al (2011) Nitrate reduction using nanosized zero-valent iron supported by polystyrene resins: Role of surface functional groups. *Water Res* 45(6):2191–2198. <https://doi.org/10.1016/j.watres.2011.01.005>
  116. Singh A, Singh K (2016) Evaluation of phosphate removal capacity of Fe<sub>3</sub>O<sub>4</sub>-ZVINPs from aqueous solution: optimization using response surface analysis. *Res Chem Intermed*. <https://doi.org/10.1007/s11164-016-2543-6>
  117. Eljamil O, Khalil AME, Sugihara Y, Matsunaga N (2016) Phosphorus removal from aqueous solution by nanoscale zero valent iron in the presence of copper chloride. *Chem Eng J* 293:225–231. <https://doi.org/10.1016/j.cej.2016.02.052>
  118. Wang H, Zou Z, Xiao X, Chen D, Yang K (2016) Reduction of highly concentrated phosphate from aqueous solution using pectin-nanoscale zerovalent iron (PNZVI). *Water Sci Technol* 73(11):2689–2696. <https://doi.org/10.2166/wst.2016.106>

119. Zhao L, Ji Y, Kong D, Lu J, Zhou Q, Yin X (2016) Simultaneous removal of bisphenol A and phosphate in zero-valent iron activated persulfate oxidation process. *Chem Eng J* 303:458–466. <https://doi.org/10.1016/j.cej.2016.06.016>
120. Sleiman N, Deluchat V, Wazne M, Mallet M, Courtin-Nomade A, Kazpard V et al (2017) Phosphate removal from aqueous solutions using zero valent iron (ZVI): Influence of solution composition and ZVI aging. *Colloids Surf A* 514:1–10. <https://doi.org/10.1016/j.colsurfa.2016.11.014>
121. Salam MA, Fageeh O, Al-Thabaiti SA, Obaid AY (2015) Removal of nitrate ions from aqueous solution using zero-valent iron nanoparticles supported on high surface area nanographenes. *J Mol Liq* 212:708–715. <https://doi.org/10.1016/j.molliq.2015.09.029>
122. Wu Y, Zhang J, Tong Y, Xu X (2009) Chromium(VI) reduction in aqueous solutions by Fe<sub>3</sub>O<sub>4</sub>-stabilized Fe<sup>0</sup> nanoparticles. *J Hazard Mater* 172:1640–1645. <https://doi.org/10.1016/j.jhazmat.2009.08.045>
123. Bajpai S, Gupta SK, Dey A, Jha MK, Bajpai V, Joshi S et al (2012) Application of Central Composite Design approach for removal of chromium (VI) from aqueous solution using weakly anionic resin: Modeling, optimization, and study of interactive variables. *J Hazard Mater* 227–228:436–444. <https://doi.org/10.1016/j.jhazmat.2012.05.016>
124. Wu D, Shen Y, Ding A, Qiu M, Yang Q, Zheng S (2013) Phosphate removal from aqueous solutions by nanoscale zero-valent iron. *Environ Technol* 34(17–20):2663–2669. <https://doi.org/10.1080/09593330.2013.786103>
125. Zhu Y, Wu M, Gao N, Chu W, Wang S (2016) Impacts of nitrate and electron donor on perchlorate reduction and microbial community composition in a biologically activated carbon reactor. *Chemosphere* 165:134–143. <https://doi.org/10.1016/j.chemosphere.2016.08.078>
126. Cho M, Ahn S (2012) The influence of activated carbon support on nitrate reduction by Fe(0) nanoparticles. *Korean J Chem Eng* 29(8):1057–1062. <https://doi.org/10.1007/s11814-011-0292-1>
127. Zhu H, Jia Y, Wu X, Wang H (2009) Removal of arsenic from water by supported nano zero-valent iron on activated carbon. *J Hazard Mater* 172(2):1591–1596. <https://doi.org/10.1016/j.jhazmat.2009.08.031>
128. Zhang L, Wan L, Chang N, Liu J, Duan C, Zhou Q et al (2011) Removal of phosphate from water by activated carbon fiber loaded with lanthanum oxide. *J Hazard Mater* 190(1):848–855. <https://doi.org/10.1016/j.jhazmat.2011.04.021>
129. Karimi S, Karri RR, Tavakkoli Yaraki M, Koduru JR (2021) Processes and separation technologies for the production of fuel-grade bioethanol: a review. *Environ Chem Lett*. <https://doi.org/10.1007/s10311-021-01208-9>
130. Chen L, Li F, Wei Y, Li G, Shen K, He H-J (2019) High cadmium adsorption on nanoscale zero-valent iron coated *Eichhornia crassipes* biochar. *Environ Chem Lett* 17(1):589–594. <https://doi.org/10.1007/s10311-018-0811-y>
131. Sleiman N, Deluchat V, Wazne M, Mallet M, Courtin-Nomade A, Kazpard V et al (2016) Phosphate removal from aqueous solution using ZVI/sand bed reactor: behavior and mechanism. *Water Res* 99:56–65. <https://doi.org/10.1016/j.watres.2016.04.054>
132. Fu F, Dionysiou D, Liu H (2014) The use of zero-valent iron for groundwater remediation and wastewater treatment: a review. *J Hazard Mater* 267C:194–205. <https://doi.org/10.1016/j.jhazmat.2013.12.062>
133. Murphy J, Riley JP (1962) A modified single solution method for the determination of phosphate in natural waters. *Anal Chim Acta* 27:31–36. [https://doi.org/10.1016/S0003-2670\(00\)88444-5](https://doi.org/10.1016/S0003-2670(00)88444-5)
134. Wen Z, Zhang Y, Dai C (2014) Removal of phosphate from aqueous solution using nanoscale zerovalent iron (nZVI). *Colloids Surf A* 457:433–440. <https://doi.org/10.1016/j.colsurfa.2014.06.017>
135. Sun YP, Li XQ, Cao J, Zhang WX, Wang HP (2006) Characterization of zero-valent iron nanoparticles. *Adv Coll Interface Sci* 120(1–3):47–56. <https://doi.org/10.1016/j.cis.2006.03.001>
136. Liu Y, Majetich SA, Tilton RD, Sholl DS, Lowry GV (2005) TCE Dechlorination rates, pathways, and efficiency of nanoscale iron particles with different properties. *Environ Sci Technol* 39(5):1338–1345. <https://doi.org/10.1021/es049195r>
137. Almeelbi T, Bezbaruah A (2012) Aqueous phosphate removal using nanoscale zero-valent iron. *J Nanopart Res* 14(7):900. <https://doi.org/10.1007/s11051-012-0900-y>
138. Chitrakar R, Tezuka S, Sonoda A, Sakane K, Ooi K, Hirotsu T (2006) Selective adsorption of phosphate from seawater and wastewater by amorphous zirconium hydroxide. *J Colloid Interface Sci* 297(2):426–433. <https://doi.org/10.1016/j.jcis.2005.11.011>
139. Yan L-G, Xu Y-Y, Yu H-Q, Xin X-D, Wei Q, Du B (2010) Adsorption of phosphate from aqueous solution by hydroxy-aluminum, hydroxy-iron and hydroxy-iron–aluminum pillared bentonites. *J Hazard Mater* 179(1):244–250. <https://doi.org/10.1016/j.jhazmat.2010.02.086>
140. Perassi I, Borgnino L (2014) Adsorption and surface precipitation of phosphate onto CaCO<sub>3</sub>–montmorillonite: effect of pH, ionic strength and competition with humic acid. *Geoderma* 232–234:600–608. <https://doi.org/10.1016/j.geoderma.2014.06.017>
141. Liu H, Sun X, Yin C, Hu C (2008) Removal of phosphate by mesoporous ZrO<sub>2</sub>. *J Hazard Mater* 151(2):616–622. <https://doi.org/10.1016/j.jhazmat.2007.06.033>
142. Wei X, Gao N, Li C, Deng Y, Zhou S, Li L (2016) Zero-valent iron (ZVI) activation of persulfate (PS) for oxidation of bentazon in water. *Chem Eng J* 285:660–670. <https://doi.org/10.1016/j.cej.2015.08.120>
143. Maruthamuthu P, Neta P (1978) Phosphate radicals. Spectra, acid-base equilibriums, and reactions with inorganic compounds. *J Phys Chem* 82(6):710–713. <https://doi.org/10.1021/j100495a019>
144. Lee Y, Zimmermann SG, Kieu AT, von Gunten U (2009) Ferrate (Fe(VI)) application for municipal wastewater treatment: a novel process for simultaneous micropollutant oxidation and phosphate removal. *Environ Sci Technol* 43(10):3831–3838. <https://doi.org/10.1021/es803588k>
145. Reardon EJ (1995) Anaerobic corrosion of granular iron: measurement and interpretation of hydrogen evolution rates. *Environ Sci Technol* 29(12):2936–2945. <https://doi.org/10.1021/es00012a008>
146. Ruangchainikom C, Liao C-H, Anotai J, Lee M-T (2006) Effects of water characteristics on nitrate reduction by the Fe<sup>0</sup>/CO<sub>2</sub> process. *Chemosphere* 63(2):335–343. <https://doi.org/10.1016/j.chemosphere.2005.06.049>
147. Rotzetter ACC, Kellenberger CR, Schumacher CM, Mora C, Grass RN, Loepfe M et al (2013) Combining phosphate and bacteria removal on chemically active filter membranes allows prolonged storage of drinking water. *Adv Mater* 25(42):6057–6063. <https://doi.org/10.1002/adma.201303119>
148. Zheng D, Yao R, Sun C, Zheng Y, Liu C (2021) Highly efficient low-concentration phosphate removal from effluents by recoverable La(OH)<sub>3</sub>/Foamed nickel adsorbent. *ACS Omega* 6(8):5399–5407. <https://doi.org/10.1021/acsomega.0c05489>
149. Sakulpaisan S, Vongsetskul T, Reamouppatum S, Luangkachao J, Tantirungrotechai J, Tangboriboonrat P (2016) Titania-functionalized graphene oxide for an efficient adsorptive removal of phosphate ions. *J Environ Manage* 167:99–104. <https://doi.org/10.1016/j.jenvman.2015.11.028>
150. Tofik AS, Tadesse AM, Tesfahun KT, Girma GG (2016) Fe–Al binary oxide nanosorbent: synthesis, characterization and



- phosphate sorption property. *J Environ Chem Eng* 4(2):2458–2468. <https://doi.org/10.1016/j.jece.2016.04.023>
151. Drenkova-Tuhtan A, Schneider M, Franzreb M, Meyer C, Gellermann C, SEXTL G et al (2017) Pilot-scale removal and recovery of dissolved phosphate from secondary wastewater effluents with reusable ZnFeZr adsorbent @ Fe<sub>3</sub>O<sub>4</sub>/SiO<sub>2</sub> particles with magnetic harvesting. *Water Res* 109:77–87. <https://doi.org/10.1016/j.watres.2016.11.039>
  152. Du X, Han Q, Li J, Li H (2017) The behavior of phosphate adsorption and its reactions on the surfaces of Fe–Mn oxide adsorbent. *J Taiwan Inst Chem Eng* 76:167–175. <https://doi.org/10.1016/j.jtice.2017.04.023>
  153. Rashidi Nodeh H, Sereshti H, Zamiri Afsharian E, Nouri N (2017) Enhanced removal of phosphate and nitrate ions from aqueous media using nanosized lanthanum hydrous doped on magnetic graphene nanocomposite. *J Environ Manage* 197:265–274. <https://doi.org/10.1016/j.jenvman.2017.04.004>
  154. Fang L, Wu B, Lo IMC (2017) Fabrication of silica-free superparamagnetic ZrO<sub>2</sub>@Fe<sub>3</sub>O<sub>4</sub> with enhanced phosphate recovery from sewage: performance and adsorption mechanism. *Chem Eng J* 319:258–267. <https://doi.org/10.1016/j.cej.2017.03.012>
  155. Jamali A, Hosseini C, Siboni M, Pourvakhshoori N, Poursadeghiyan M, Farrokhi M (2017) Application of ZnO-Fe<sub>3</sub>O<sub>4</sub> nano composite on the phosphate removal from aqueous solutions: optimization and statistical modeling. *Orient J Chem* 33:1744–1755. <https://doi.org/10.13005/ojc/330419>
  156. Chen X, Wang XC, Yang S (2017) La(III) coagulated graphene oxide for phosphate binding: mechanism and behaviour. *Int J Environ Stud* 74(4):586–602. <https://doi.org/10.1080/00207233.2017.1333271>
  157. Park H-S, Kwak S-H, Mahardika D, Mameda N, Choo K-H (2017) Mixed metal oxide coated polymer beads for enhanced phosphorus removal from membrane bioreactor effluents. *Chem Eng J* 319:240–247. <https://doi.org/10.1016/j.cej.2017.03.017>
  158. Kostura B, Huczala R, Ritz M, Leško J (2018) Retention of phosphates from aqueous solutions with in sol–gel-derived amorphous CaO–MgO–Al<sub>2</sub>O<sub>3</sub>–SiO<sub>2</sub> system as a model of blast furnace slag. *Chem Pap* 72(2):401–408. <https://doi.org/10.1007/s11696-017-0289-2>
  159. Chon C-M, Cho D-W, Nam I-H, Kim J-G, Song H (2018) Fabrication of Fe/Mn oxide composite adsorbents for adsorptive removal of zinc and phosphate. *J Soils Sediments* 18(3):946–956. <https://doi.org/10.1007/s11368-017-1784-3>
  160. Bai L, Yuan L, Ji Y, Yan H (2018) Effective removal of phosphate from aqueous by graphene oxide decorated with α-Fe<sub>2</sub>O<sub>3</sub>/β-Fe<sub>2</sub>O<sub>3</sub>: kinetic, isotherm, thermodynamic and mechanism study. *Arab J Sci Eng* 43(7):3611–3620. <https://doi.org/10.1007/s13369-018-3124-3>
  161. Kondalkar M, Fegade U, Attarde S, Ingle S (2018) Experimental investigation on phosphate adsorption, mechanism and desorption properties of Mn–Zn–Ti oxide trimetal alloy nanocomposite. *J Dispersion Sci Technol* 39(11):1635–1643. <https://doi.org/10.1080/01932691.2018.1459678>
  162. Li N, Tian Y, Zhao J, Zhan W, Du J, Kong L et al (2018) Ultrafast selective capture of phosphorus from sewage by 3D Fe<sub>3</sub>O<sub>4</sub>@ZnO via weak magnetic field enhanced adsorption. *Chem Eng J* 341:289–297. <https://doi.org/10.1016/j.cej.2018.02.029>
  163. Awual MR, Yaita T, El-Safty SA, Shiwaku H, Okamoto Y, Suzuki S (2013) Investigation of palladium(II) detection and recovery using ligand modified conjugate adsorbent. *Chem Eng J* 222:172–179. <https://doi.org/10.1016/j.cej.2013.02.058>
  164. Cui H-J, Cai J-K, Zhao H, Yuan B, Ai C-L, Fu M-L (2014) Fabrication of magnetic porous Fe–Mn binary oxide nanowires with superior capability for removal of As(III) from water. *J Hazard Mater* 279:26–31. <https://doi.org/10.1016/j.jhazmat.2014.06.054>
  165. Ren Y, Yang J, Li J, Lai B (2017) Strengthening the reactivity of FeO(Fe/Cu) by premagnetization: Implications for nitrate reduction rate and selectivity. *Chem Eng J* 330:813–822. <https://doi.org/10.1016/j.cej.2017.08.029>
  166. Liu Y, Sheng X, Dong Y, Ma Y (2012) Removal of high-concentration phosphate by calcite: effect of sulfate and pH. *Desalination* 289:66–71. <https://doi.org/10.1016/j.desal.2012.01.011>
  167. Rodrigues LA, da Silva MLCP (2009) An investigation of phosphate adsorption from aqueous solution onto hydrous niobium oxide prepared by co-precipitation method. *Colloids Surf A* 334(1):191–196. <https://doi.org/10.1016/j.colsurfa.2008.10.023>
  168. Almanassa IW, Kochkodan V, McKay G, Atieh MA, Al-Ansari T (2021) Review of phosphate removal from water by carbonaceous sorbents. *J Environ Manage* 287:112245. <https://doi.org/10.1016/j.jenvman.2021.112245>
  169. Abebe B, Tadesse AM, Kebede T, Teju E, Diaz I (2017) Fe–Al–Mn ternary oxide nanosorbent: synthesis, characterization and phosphate sorption property. *J Environ Chem Eng* 5(2):1330–1340. <https://doi.org/10.1016/j.jece.2017.02.026>
  170. Szlachta M, Chubar N (2013) The application of Fe–Mn hydrous oxides based adsorbent for removing selenium species from water. *Chem Eng J* 217:159–168. <https://doi.org/10.1016/j.cej.2012.11.100>
  171. Drenkova-Tuhtan A, Schneider M, Mandel K, Meyer C, Gellermann C, SEXTL G et al (2016) Influence of cation building blocks of metal hydroxide precipitates on their adsorption and desorption capacity for phosphate in wastewater—a screening study. *Colloids Surf A* 488:145–153. <https://doi.org/10.1016/j.colsurfa.2015.10.017>
  172. Yoon S-H, Lee C-H, Kim K-J, Fane AG (1998) Effect of calcium ion on the fouling of nanofilter by humic acid in drinking water production. *Water Res* 32(7):2180–2186. [https://doi.org/10.1016/S0043-1354\(97\)00416-8](https://doi.org/10.1016/S0043-1354(97)00416-8)
  173. Long F, Gong J-L, Zeng G-M, Chen L, Wang X-Y, Deng J-H et al (2011) Removal of phosphate from aqueous solution by magnetic Fe–Zr binary oxide. *Chem Eng J* 171(2):448–455. <https://doi.org/10.1016/j.cej.2011.03.102>
  174. Morin-Crini N, Lichtfouse E, Torri G, Crini G (2019) Applications of chitosan in food, pharmaceuticals, medicine, cosmetics, agriculture, textiles, pulp and paper, biotechnology, and environmental chemistry. *Environ Chem Lett* 17(4):1667–1692. <https://doi.org/10.1007/s10311-019-00904-x>
  175. Brião GDV, de Andrade JR, daSilva MGC, Vieira MGA (2020) Removal of toxic metals from water using chitosan-based magnetic adsorbents. A review. *Environ Chem Lett* 18(4):1145–1168. <https://doi.org/10.1007/s10311-020-01003-y>
  176. Bozorgpour F, Ramandi HF, Jafari P, Samadi S, Yazd SS, Aliabadi M (2016) Removal of nitrate and phosphate using chitosan/Al<sub>2</sub>O<sub>3</sub>/Fe<sub>3</sub>O<sub>4</sub> composite nanofibrous adsorbent: comparison with chitosan/Al<sub>2</sub>O<sub>3</sub>/Fe<sub>3</sub>O<sub>4</sub> beads. *Int J Biol Macromol* 93:557–565. <https://doi.org/10.1016/j.jbiomac.2016.09.015>
  177. Yazdani MR, Virolainen E, Conley K, Vahala R (2017) Chitosan-Zinc(II) complexes as a bio-sorbent for the adsorptive abatement of phosphate: mechanism of complexation and assessment of adsorption performance. *Polymers*. <https://doi.org/10.3390/polym10010025>
  178. Zavareh S, Behrouzi Z, Avanes A (2017) Cu (II) binded chitosan/Fe<sub>3</sub>O<sub>4</sub> nanocomposite as a new biosorbent for efficient and selective removal of phosphate. *Int J Biol Macromol* 101:40–50. <https://doi.org/10.1016/j.jbiomac.2017.03.074>
  179. Kumar IA, Viswanathan N (2017) Development of multivalent metal ions imprinted chitosan biocomposites for phosphate sorption. *Int J Biol Macromol* 104:1539–1547. <https://doi.org/10.1016/j.jbiomac.2017.02.100>
  180. Kim JH, Kim SB, Lee SH, Choi JW (2018) Laboratory and pilot-scale field experiments for application of iron oxide

- nanoparticle-loaded chitosan composites to phosphate removal from natural water. *Environ Technol* 39(6):770–779. <https://doi.org/10.1080/09593330.2017.1310937>
181. Banu HT, Meenakshi S (2017) One pot synthesis of chitosan grafted quaternized resin for the removal of nitrate and phosphate from aqueous solution. *Int J Biol Macromol* 104:1517–1527. <https://doi.org/10.1016/j.ijbiomac.2017.03.043>
182. Rojsitthisak P, Burut-Archanai S, Pothipongsa A, Powtongsook S (2017) Repeated phosphate removal from recirculating aquaculture system using cyanobacterium remediation and chitosan flocculation. *Water Environ J* 31(4):598–602. <https://doi.org/10.1111/wej.12288>
183. Józwiak T, Filipkowska U, Szymczyk P, Rodziewicz J, Mielcarek A (2017) Effect of ionic and covalent crosslinking agents on properties of chitosan beads and sorption effectiveness of Reactive Black 5 dye. *React Funct Polym* 114:58–74. <https://doi.org/10.1016/j.reactfunctpolym.2017.03.007>
184. Huang Y, Lee X, Grattieri M, Macazo FC, Cai R, Minteer SD (2018) A sustainable adsorbent for phosphate removal: modifying multi-walled carbon nanotubes with chitosan. *J Mater Sci* 53(17):12641–12649. <https://doi.org/10.1007/s10853-018-2494-y>
185. Aswin Kumar I, Viswanathan N (2018) Development and reuse of amine-grafted chitosan hybrid beads in the retention of nitrate and phosphate. *J Chem Eng Data* 63(1):147–158. <https://doi.org/10.1021/acs.jced.7b00751>
186. Thagira Banu H, Karthikeyan P, Meenakshi S (2018) Lanthanum (III) encapsulated chitosan-montmorillonite composite for the adsorptive removal of phosphate ions from aqueous solution. *Int J Biol Macromol* 112:284–293. <https://doi.org/10.1016/j.ijbiomac.2018.01.138>
187. Bhatnagar A, Sillanpää M (2009) Applications of chitin- and chitosan-derivatives for the detoxification of water and wastewater—a short review. *Adv Coll Interface Sci* 152(1):26–38. <https://doi.org/10.1016/j.cis.2009.09.003>
188. Wan Ngah WS, Teong LC, Hanafiah MAKM (2011) Adsorption of dyes and heavy metal ions by chitosan composites: a review. *Carbohydr Polym* 83(4):1446–1456. <https://doi.org/10.1016/j.carbpol.2010.11.004>
189. Kumar IA, Viswanathan N (2017) Fabrication of metal ions cross-linked alginate assisted biocomposite beads for selective phosphate removal. *J Environ Chem Eng* 5(2):1438–1446. <https://doi.org/10.1016/j.jece.2017.02.005>
190. Kalaruban M, Loganathan P, Shim WG, Kandasamy J, Naidu G, Nguyen TV et al (2016) Removing nitrate from water using iron-modified Dowex 21K XLT ion exchange resin: batch and fluidised-bed adsorption studies. *Sep Purif Technol* 158:62–70. <https://doi.org/10.1016/j.seppur.2015.12.022>
191. Nur T, Shim WG, Loganathan P, Vigneswaran S, Kandasamy J (2015) Nitrate removal using Purolite A520E ion exchange resin: batch and fixed-bed column adsorption modelling. *Int J Environ Sci Technol* 12(4):1311–1320. <https://doi.org/10.1007/s13762-014-0510-6>
192. Filipkowska U, Józwiak T (2013) Application of chemically-cross-linked chitosan for the removal of Reactive Black 5 and Reactive Yellow 84 dyes from aqueous solutions. *J Polym Eng* 33:735–747. <https://doi.org/10.1515/polyeng-2013-0166>
193. Filipkowska U, Józwiak T, Szymczyk P (2014) Application of cross-linked chitosan for phosphate removal from aqueous solutions. *Progress Chem Appl Chitin Deriv* XiX:5–14
194. Leduc J-F, Leduc R, Cabana H (2014) Phosphate adsorption onto chitosan-based hydrogel microspheres. *Adsorpt Sci Technol* 32(7):557–569. <https://doi.org/10.1260/0263-6174.32.7.557>
195. Qin K, Li F, Xu S, Wang T, Liu C (2017) Sequential removal of phosphate and cesium by using zirconium oxide: a demonstration of designing sustainable adsorbents for green water treatment. *Chem Eng J* 322:275–280. <https://doi.org/10.1016/j.cej.2017.04.046>

**Publisher's Note** Springer Nature remains neutral with regard to jurisdictional claims in published maps and institutional affiliations.